Sudan University of Science and Technology

College of Post Graduate Studies

A Selective Window for Indoor Thermal Comfort in Building

نافذة إنتقائية لتوفير درجة حرارة مريحة بالداخل

A thesis submitted for fulfillment of the requirements for the degree of Ph.D. in physics

By:

Manahil Hassan Mohammed Ahmed Balal

Supervisor:

Prof. Mohammed Osman Sid Ahmed

آيات من القرآن الكريم

بسم الله الرحمن الرحيم

[هُوَ الَّذِي جَعَلَ الشَّمْسَ ضِيَاء وَالْقَمَرَ نُوراً وَقَدَّرَهُ مَنَازِلَ لِتَعْلَمُواْ عَدَدَ السِّنِينَ وَالْحِسَابَ مَا خَلَقَ اللّهُ ذَلِكَ إِلاَّ بِالْحَقِّ يُفَصِّلُ الآيَاتِ لِقَوْمٍ يَعْلَمُونَ] يونس: ٥.

[وَجَعَلَ الْقَمَرَ فِيهِنَّ نُوراً وَجَعَلَ الشَّمْسَ سِرَاجاً] نوح: ١٦.

Dedication

To my mother,,,,,,,

To my father,,,,,,,

My brother and sisters,,,,,,

To my friends,,,,,,,,

Their moral support has been incentive to this hard work.

ACKNOWLEDGMENT

First of all I would like to thanks God a lot for making this work possible**.**

I would like to express my deepest gratitude to my Supervisor **Prof. Mohamed Osman Sid Ahmed**, for his excellent guidance, caring, patience, motivation, enthusiasm, and immense knowledge. His guidance helped me in all the time of research and writing of this thesis. I do appreciate the attention and timely response he gave whenever it was in need of help, his wide and in-depth knowledge in material science and instrumentation, he gave me the courage and ability I needed most in doing this work.

I'm grateful to **Dr**. **Daniel**, who gave me conducive learning environment during my stay as a student at University of Witwatersrand, South Africa. I would like to thank my father who inspires and help me since my childhood. My great thanks also to my brother Engineer. Mohamed Hassan who traveled with me to South Africa.

My profound gratitude extent to my family; for their support and their encouragement.

Finally, I would like to send my regards and thanks to **my fiancé** , **Abdillah Elamin** , who always cheering and standing by me through the good times and bad ones..

TABLE OF CONTENTS

LIST OF TABLES

LIST OF FIGURES

ABSTRACT

Buildings in Sudan experience significant amount of heat gain through windows and this affects the thermal comfort of buildings' occupants. There are many commercially available smart windows that control the reflection and transmission of visible light and infrared radiation, but they suffer from the high cost, low transmission of the visible light and some of them require external power for operation.

The proposed glazing is relatively simple and it does not need any external source of energy to control its optical properties. Rigorous coupled-wave analysis (RCWA) has been used to design the glazing. The glazing consists of Induim Tin Oxide (ITO) and four periodic pairs of Si/SiO_2, deposited on a glass sheet. The optimum thicknesses of Indium tin oxide ITO, Si and SiO_2, obtained from the simulation, are (0.1 , 0.15 and o.4) μm respectively. The simulation has also shown that the filter transmits 70-80% of the visible light and reflects almost all the infrared radiation.

The preparation of the filter and the testing has been performed at the laboratories of the Faculty of Science, University of Witwatersrand (Wits), South Africa. Magnetron sputtering technique has been used for the fabrication. Indium tin oxide (ITO), silicon (Si) and silicon dioxide (SiO_2) have been used as sputtering targets. The magnetron sputtering system has been used to deposit a thin film from the sputtering targets onto the substrate. The fabricated filter has transmitted about 78% of the incident light and reflected almost all the infrared radiation. The experimental results have been almost typical to the simulation results.

المستخلص

تكتسب المباني في السودان طاقة حرارية كبيرة من خلال النوافذ، وهذا يؤثر على راحة السكان بداخل المبني .هنالك العديد من النوافذ الذكية المتاحة تجارياً التي تتحكم في إنعكاس وإنفاذ الضوء المرئي والأشعة تحت الحمراء، لكنها تعاني من التكلفة العالية وتتسم بإنخفاض إنتقال الضوء المرئي وبعضها يتطلب طاقة خارجية للتشغيل . تركيب الزجاج المقترح بسيط نسبيا ولا يحتاج إلى أي مصدر خارجي للطاقة للتحكم في خصائصه البصرية . تم تصميم النوافذ الانتقائية باستخدام برنامج التحليل الموجي المقترن بقوة . وتتكون النافذة من أُكسيد الانديوم والصفيح (ITO) وأربع طبقات دورية من السليكون وأُكسيد السليكون (Si/SiO_2) موضوعه علي شريحة زجاجية. تم الحصول علي السمك الأمثل من ITO،Si،SiO_2 من المحاكاة، وهي (٠.١، ٠.١٥ و ٠.٤) ميكرون، على التوالي . وقد أظهرت المحاكاة أيضا أن المرشح ينفذ ٧٠–٨٠٪ من الضوء المرئي ويعكس تقريبا كل الأشعة تحت الحمراء . وقد تم إعداد المرشح والاختبار في مختبرات كلية العلوم، جامعة ويتس، جنوب أفريقيا .وقد استخدمت تقنية الرش المغنطيسي لتصنيع طبقة رقيقة من مصادر الرش على الركيزة . المرشح المصنع ينفذ حوالي ٧٨٪ من الضوء الساقط ويعكس معظم الاشعه تحت الحمراء.النتائج التجريبية كانت نموذجية تقريبا لمحاكاة النتائج.

Chapter1

Introduction

1.1 Solar Radiation

The sun is a 1.39 x 106 km diameter sphere comprised of many layers of gases, which are progressively hotter towards its centre. It has an equivalent black body temperature of about 5760 ^{o}K at the surface [1]. The sun is, in effect, a continuous fusion reactor with its constituent gases, retained by gravitational forces. This energy is produced in the interior of the sun, at temperatures of many millions of degrees .The rate of energy emission is 3.8 x 10^{23} KW, which results from the conversion of about 4.3 x 10^{9} kg/s of its mass into energy, out which only
1.7 x 10^{14} kW reaches the earth surface. The solar energy is transmitted to the earth as an electromagnetic radiation, the maximum of which is in the visible range of the spectrum (0.3-0.78μm).The radiation power emitted increases with the fourth power of the absolute temperature as given by Stefan Boltzmann law. The amount of solar radiation near the earth surface is called the solar constant and is equal to 1.353 kW/ m^2 [1] .

Modern architecture tends to increase the window to wall ratio for aesthetic purposes. Given the concerns on energy saving and low carbon, people can use the solar energy to decrease the electricity consumption for lighting.

1.2The Solar Spectrum

The sun provides the energy needed to sustain life in our solar system .In one hour, the Earth receives enough energy from the sun to meet its energy needs for nearly a

year[2]. In other words, this is about 5000 times the input to the energy budget of the Earth from all other sources.

The sun is composed of a mixture of gases with a predominance of hydrogen. As the sun converts hydrogen to helium in a massive thermonuclear fusion reaction, mass is converted to energy according to Einstein' s famous formula:

$$E = mc^2 \qquad (1.1)$$

where m is the mass and c is the speed of light in vacuum.

This energy is radiated away from the sun uniformly in all directions, in close agreement with Planck's blackbody radiation formula:

$$W_\lambda = \frac{2\pi hc^2\lambda^{-5}}{e^{\frac{hc}{\lambda kT}}-1}(w/m^2/unitwavelenghtinmeters) \qquad (1.2)$$

Where

h = 6.63×10^{-34} wattsec^2 (Plank 's constant ,and

k = 1.38×10^{-23} joules/k (Boltzmann 's constant)

Equation 1.2 yields the energy density at the surface of the sun in w/m^2 /unit wavelength. By the time this energy has traveled 150 million km to the Earth, the total extraterrestrial energy density decreases to 1367 W/ m^2 and is often referred to as the solar constant [2].

Figure 1.1 shows plots of Planck's blackbody radiation formula for several different temperatures, along with the extraterrestrial solar spectrum. At lower temperatures, nearly all of the spectrum lies outside the visible range in the

infrared range. At even higher temperatures, the color shifts to ward blue, and at lower temperatures, the color shifts toward read. The extraterrestrial solar spectrum indicates that the sun can be reasonably approximated as a blackbody radiator.

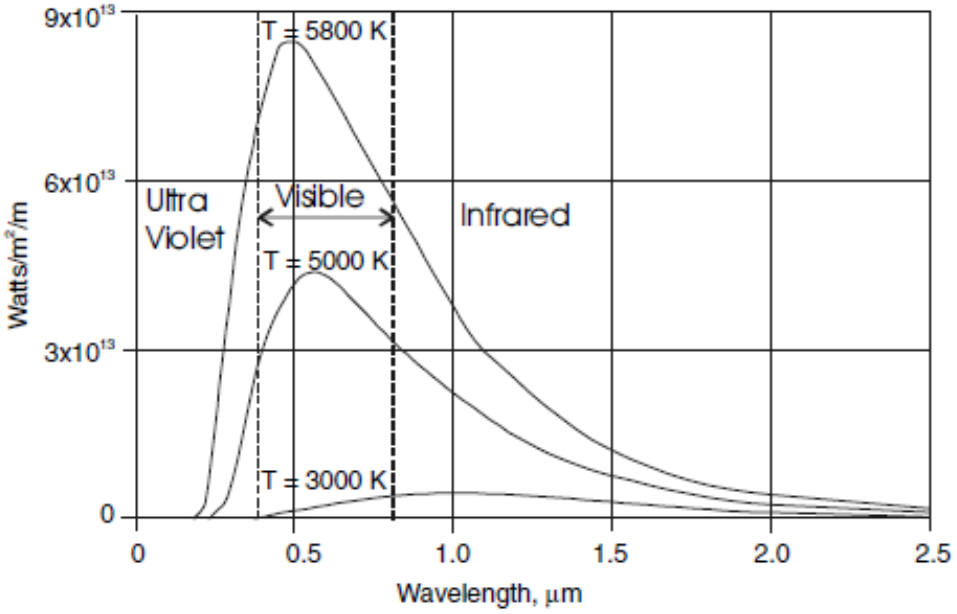

Figure1.1: Blackbody radiation spectra for temperature of 3000K, 5000K and 5800[2]

Most sources of light are not perfect blackbody sources. Reasonable approximation of blackbody spectra are obtained from sources that emit light as a result of heating a filament to a high temperature. But to a perfect radiator, the object must also be a perfect absorber of light, which is not the case for common light sources.

As sunlight enters the Earth' s atmosphere some is absorbed, some is scattered and some passes through unaffected by the molecules in the atmosphere and is either absorbed or reflected by objects at ground level.

Different molecules do different things. Water vapor, carbon dioxide and ozone, have several significant absorption wavelengths. Ozone plays an import role by absorbing a significant amount of radiation in the ultraviolet region of the spectrum, while water vapor and carbon dioxide absorption primarily in the visible and infrared parts of the spectrum.

Absorbed sunlight increases the energy of the absorbing molecules, thus raising their temperature. Scattered sunlight responsible for light entering north-facing windows when the sun is in the south. Scattered sunlight, in fact, is what makes the sky blue. Without atmosphere and its ability to scatter sunlight, the sky would appear black, such as it doses on the moon. Direct sunlight consists of parallel rays, which are necessary if the light is to be focused. Sunlight that reaches the Earth's surface without scattering is called direct or beam radiation. Scattered sunlight is called diffuse radiation.

The amount of sunlight either absorbed or scattered depends on the length of path through the atmosphere. This path length is generally compared with a vertical path directly to sea level, which is designated as air mass=1(AMI). In general, the air mass through which sunlight passes is proportional to the secant of the zenith angle,θ_z.The zenith angle is the angle measured between the direct beam and the vertical.

At AMI, after absorption has been accounted for, the intensity of the global radiation is generally reduced from 1367W/m^2 at the top of the atmosphere to just over 1000W/m^2 at sea level [2].

On the average, over the surface of the Earth, an amount of heat is reradiated into space at night that is just equal to the amount absorbed from the sun during the day. As long as this steady state condition persists, the average temperature of the Earth will remain constant. However, if for any reasons the amount of heat absorbed is not equal to the amount reradiated, the planet will either cool down or

heat up. This delicate balance can be upset by events such as volcanoes that fill the atmosphere with fine ash that reflects the sunlight away from the Earth, thus reducing the amount of incident sunlight. The balance can also be upset by gas such as carbon dioxide and methane, which are mostly transparent to short wavelength (visible) radiation, but more absorbing to long wavelength (infrared) radiation.

The natural compensation mechanism is green plants on land and under water. Through the process of photosynthesis, they use sunlight and carbon dioxide to produce plant fiber and oxygen, which is released to the atmosphere.

1.3The Orbit and Rotation of the Earth

The polar axis of the Earth is inclined by an angle of 23.45^0 to the plane of the Earth orbit about the sun. This inclination is what causes the sun to be higher in the sky in the summer than in the winter. It is also the cause of longer summer sunlight hours and shorter winter sunlight hours. Figure 1.2 shows the Earth orbit around the sun with the inclined polar axis. On the first day of Northern Hemisphere summer, the sun appears vertically above the Tropic of Cancer, which is latitude 23.45^0 N of the equator. On the first day of winter, the sun appears vertically above the Tropic of Capricorn, which is latitude 23.45^0 S of the equator. On the first day of spring and the first day of fall, the sun is directly above the equator. From fall to spring, the sun is south of the equator and from spring to fall the sun is north of the equator. The angle of deviation of the sun from directly above the equator is called the declination, δ .If angles north of the equator are considered as positive and angles south of the equator are considered negative, then at any given day of the years, n, the declination can be found from the equation :

$$\delta = 23.45^0 sin\left[\frac{360(n-80)}{365}\right] \quad (1.3)$$

This formula, of course, is only a good approximation, since the year is not exactly 365 days long and the first day of spring is not always the 80th day of the year. In any case, to determine the location of the sun in the sky at any time of day at any time of year at any location on the planet, the declination is an important parameter.

The zenith angle is related to the declination by:

$cos\theta_z = sin\delta\ sin\varphi + cos\delta\ cos\varphi \cos\omega$ (1.4)

where φ is the latitude and ω is the hour angle.

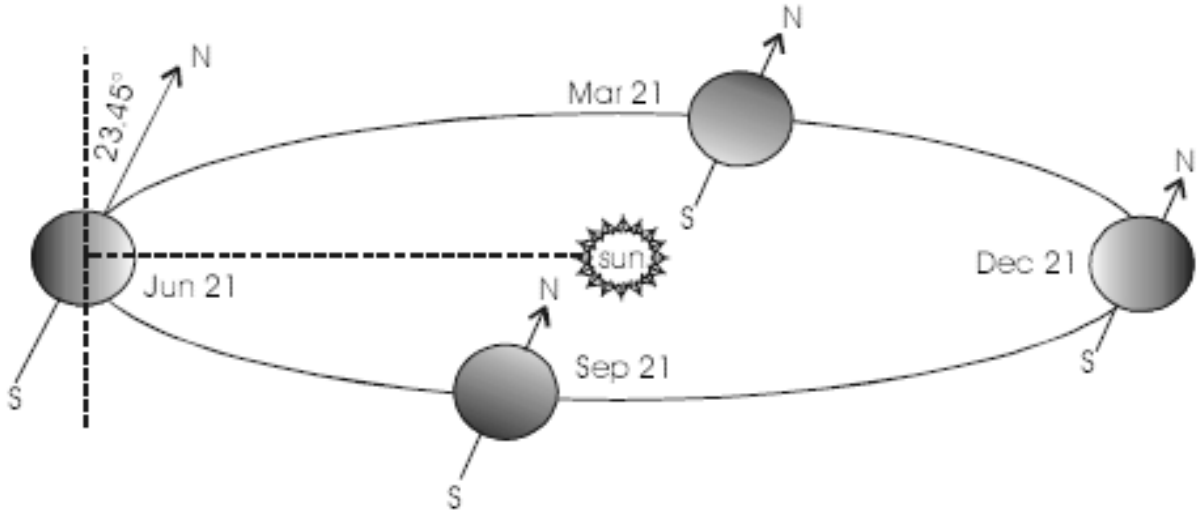

Figure1.2 : The orbit of the earth and the declination at different time of the year[2]

1.4 Solar Energy in Sudan

As it is illustrated in Figure.1.3, the solar resource is available almost everywhere. The average daily solar irradiation is 5.8 – 7.2 kWh/m^2,[3]. The maximum, 7.2 kWh/m^2, is in the north west of the country, while the minimum, 5.8 kWh/m^2 , is in the south west.

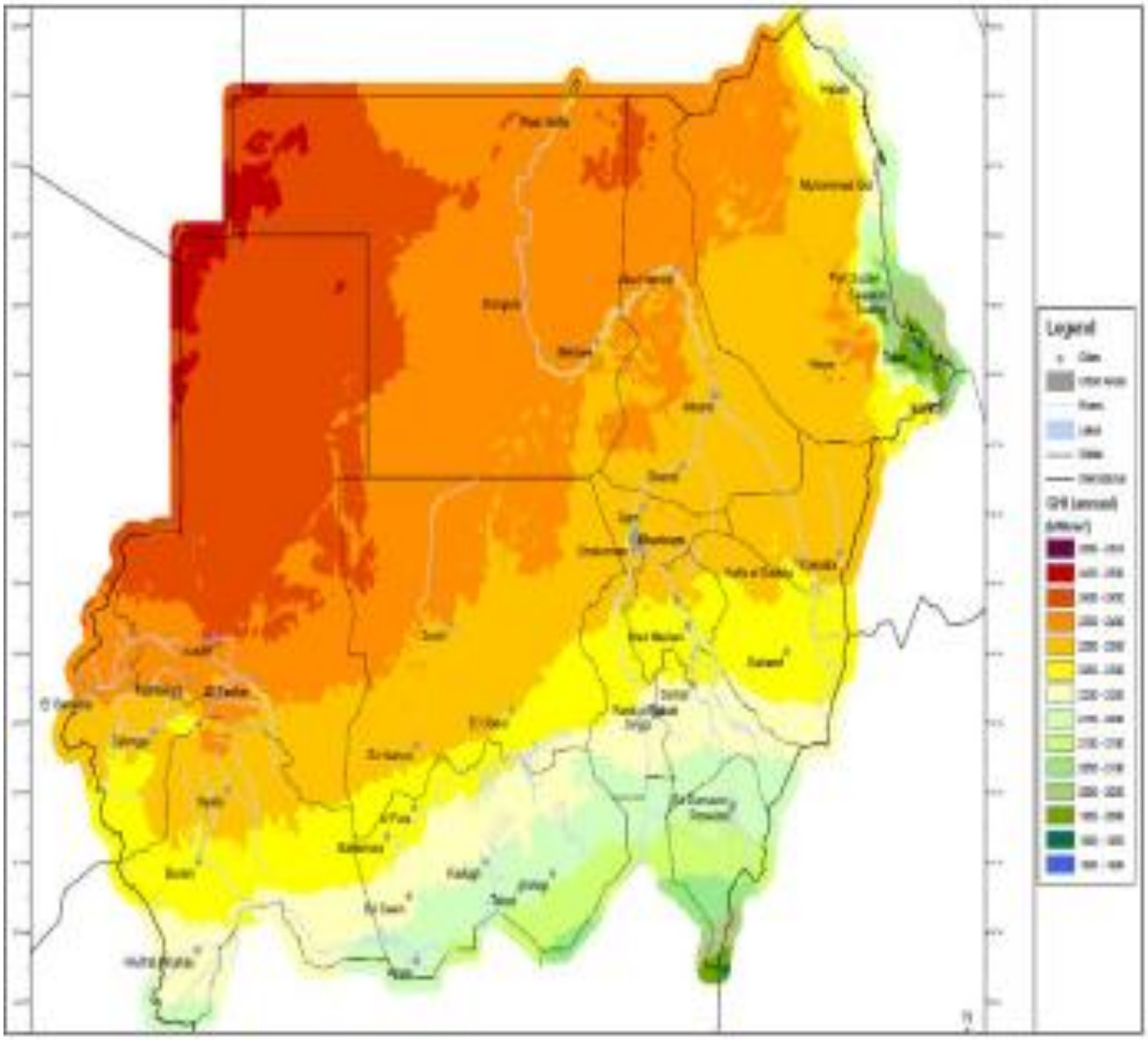

Figure:1.3: Solar radiation in Sudan.

1.5 Temperature in Sudan

In the north, the climate is desert, and in particular the northernmost area, near the border with Egypt, is one of the driest and sunniest in the world. Winter temperatures are pleasantly warm by day and cool at night, even cold at times, especially in the far north, where it can occasionally drop to around freezing. The rest of the year is rather hot, with highs around 40 °C from May to October, but with records of 50/52 °C. The wind can raise sandstorms at any time of the year [4].

Table 1.1(a) : Average températures at WadiHalfa

WadiHalfa	Jan	Feb	Mar	Apr	May	Jun	Jul	Aug	Sep	Oct	Nov	Dec
Min(°C)	7	8	12	16	21	23	23	23	22	19	14	9
Max(°C)	23	26	31	36	40	41	41	40	38	36	30	25

Khartoum is located at 400 meters above sea level, where the White Nile and the Blue Nile meet. With an average annual temperature of 30 °C, Khartoum is one of the hottest capitals in the world. In winter it's hot: highs are around 31 °C even in January, but sometimes it can get cold at night, in fact the cold record is only 1 °C; in spring the temperatures increase rapidly, so that they reach 40 °C already in April; in April and May sometimes the temperature have reached
47 °C.

Table 1.1(b) : Average températures at Khartoum

Khartoum	Jan	Feb	Mar	Apr	May	Jun	Jul	Aug	Sep	Oct	Nov	Dec
Min(°C)	16	17	20	24	27	28	26	26	26	26	21	17
Max(°C)	31	33	37	40	42	41	39	38	39	39	35	32

In July and August, under the influence of the monsoon, which brings a bit of rain, the temperature decreases slightly, but it remains very high, around 38/39 °C, and then between October and November, at the end of the monsoon, it increases slightly again, rising to 39/40 °C. This high temperature requires development of suitable architecture for the buildings and finding means of reducing the heat through the windows of houses and vehicles.

1.6 Electricity Generation and Consumption

The total Generated electricity in Sudan is about 11.665 GWh, Figure.1.4. 23% is thermal and 77% is hydro. The household Sector consumes about 52% of the total electricity consumption, Figure.1.5[3]. This is mainly for lighting and cooling. This can be greatly reduced by using spectrally selective windows, in the houses, which reflect the heat and transmit the light.

The Ministry of Water Resources, Irrigation and Electricity in Sudan prepared many plans for electricity generation from renewable energy (RE). In 2031, RE will represent 29.3% of the installed capacity, Figure. 1.6.

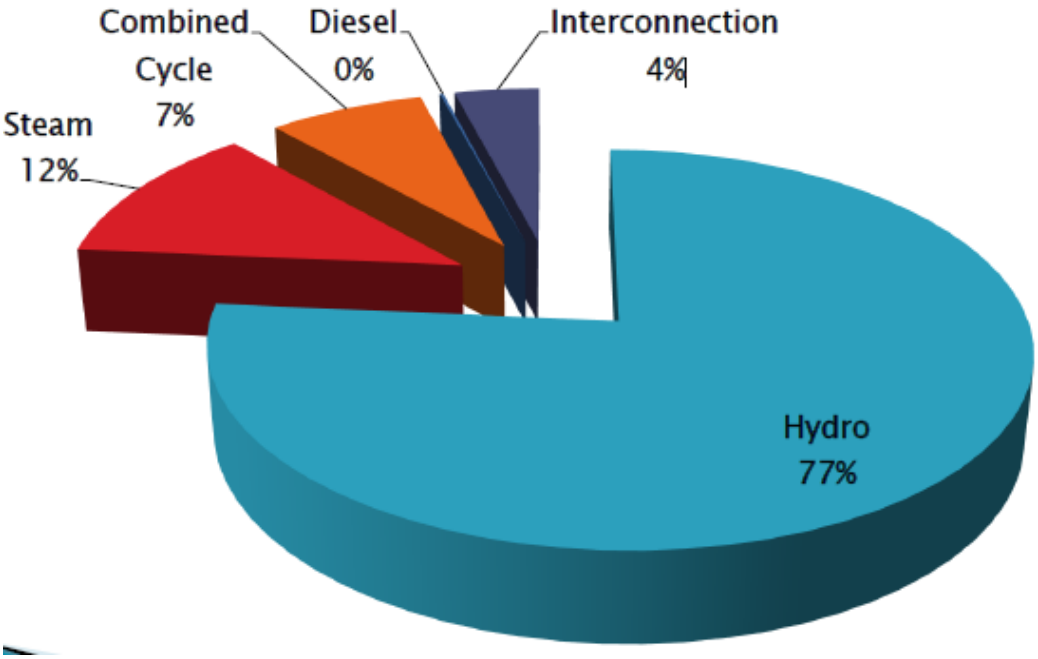

Figure.1.4: total Generated electricity in Sudan.

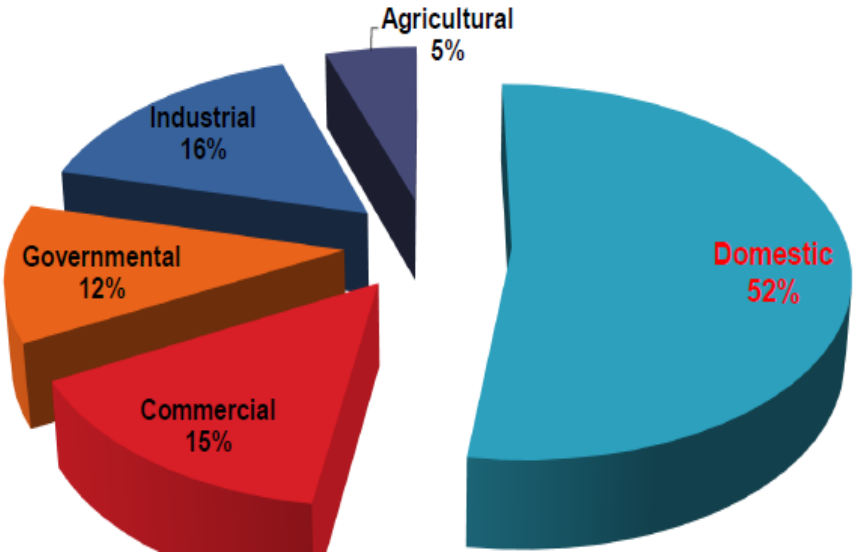

Figure.1.5 Energy consumption in Sudan.

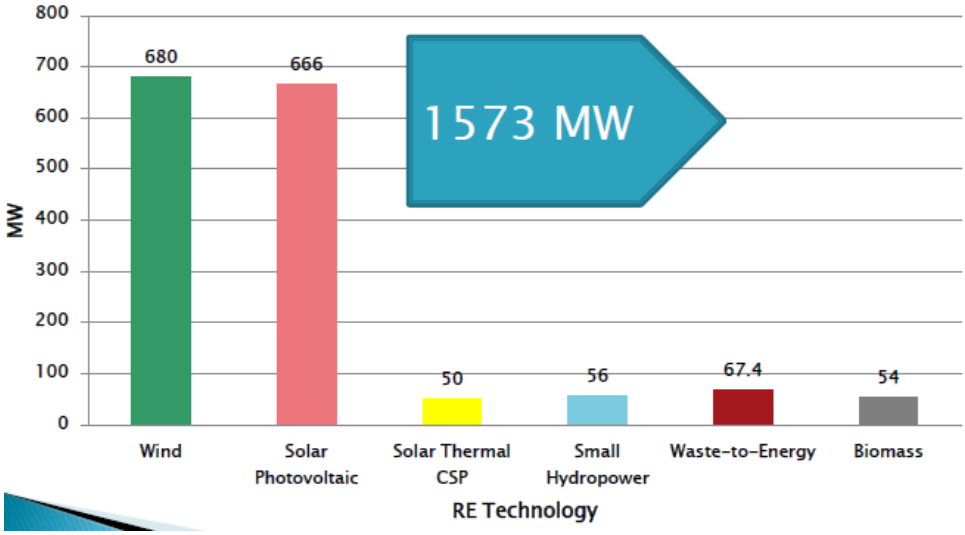

Figure1.6: Future plan for electricity generation from RE.

1.7 Motivation

At present, 23% of the generated electricity in Sudan is from thermal power plants. Emission of CO_2 and N_2O from these plants contributes to the greenhouse gases and at the same time represents an air pollution source that affects the health of the population. The indoor environment is controlled artificially. Cooling and lighting in buildings consume nearly 52% of the generated electricity. This load can be greatly reduced by using efficient and cheap windows which transmit the visible light from the sun and reflect the heat.

1.8 Objective of the Study

The main objective of this study is to design and fabricate a cheap and efficient prototype selective window, suitable for hot climates. The window has to transmit

the visible light, to reduce the electricity consumption for lighting, and reflect the infrared radiation, to reduce electricity consumption for the cooling.

1.9 Layout of the Thesis

In chapter one we considered solar energy and electricity generation. This is because solar energy is directly related to the thermal performance of buildings and electricity is consumed for lighting and cooling the buildings. Chapter two deals with human thermal comfort. The basic information about human comfort and the factors that influence the thermal comfort were discussed. Chapter three deals with smart window technologies. Presently, the most common windows are the electrochromic and thermochromic. Chapter four is devoted to the simulation for optimizing the design of the proposed window. Rigorous coupled-wave analysis was used for optimizing the dimensions of the different layers of the filter. Chapter five deals with the instrumentations for preparing and measuring the thicknesses of the different layers of (Si/SiO_2) and the instruments for measuring the optical performance of the filter. Chapter six describes the design, construction of the test rig, the material, equipment and procedures adopted for each experimental part of the study. It explains the design and construction of the test rig, its components and their functions, the chapter also deals with the experimental procedure and the analytical techniques used to assess the performance of the test rig. Chapter seven deals with the results obtained from the tests. Chapter eight is devoted to the conclusion and recommendations.

Chapter Two

Human thermal comfort

2.1 Introduction

The human comfort depends upon physiological and psychological conditions. Thus, it is difficult to define the term human comfort. There are many definitions given for this term by different bodies.

The most commonly accepted definition, from the subject point of view, is the one given by the American Society of Heating, Refrigeration and Air Conditioning Engineers (ASHRAE) [5], which states: human comfort is that condition of mind, which expresses satisfaction with the thermal environment and is assessed by subjective evaluation. The factors that define the conditions for thermal comfort are:

• Metabolic rate (the rate of transformation of chemical energy into heat and mechanical work by metabolic activities within an organism).

•Clothing insulation.

• Air temperature

•Radiant temperature.

•Air speed.

•Humidity

2.2 Indoor thermal comfort

Urbanized areas worldwide have increased and according to the United Nations it is expected that more than 70% of the world population will be located in urban centers by 2050[6]. According to the world development indicators, 85% of the population will be located in developing countries in 2030. This growth is leading to an increase in the urban density of buildings, especially in the city center, thereby influencing the characteristics of indoor environments that increasingly rely on artificial systems to operate satisfactorily. The increased amount of time people spend inside buildings is significant. As architects and engineers think of ways to improve the user's environmental comfort while improving the performance of buildings, it is imperative they consider that people spend between 80% and 90% of their days indoors[6].In developed countries, the building sector (residential, commercial and public) uses between 20% and 40% of final energy consumption.

Worldwide, buildings consume about 70% of final energy consumption through air conditioning systems and artificial lighting. In Sudan the electricity consumption in building for cooling and lighting is about 52% of the generated electricity [3].

Specifically, thermal comfort and energy efficiency were the focus of multiple studies. In recent years, the field of research in thermal comfort has attracted the attention of many researchers around the world, perhaps partially due to the increased public discussion about climate change.

Overall thermal comfort and the assessment of indoor environmental quality do not depend solely on physical parameters. The human body's physiological and psychological responses to the environment are dynamic and integrate various physical phenomena that interact with the space (light, noise, vibration, temperature, humidity, etc.).The specialization of existing standards to study and

improve each of the environments is an example of the difficulty in the whole evaluation of environments.

Ricardo et al [6] reviewed the papers published in 10 years that examine the various subareas of research related to human thermal comfort. The results of review showed broader ranges of indoor temperatures. Between 19.5 and 25.5 ^{0}C, buildings may operate in free-running mode. Above 25.5 ^{0}C up to 28.0 ^{0}C and even 30.0 ^{0}C, the use of ceiling fans and personally controlled fans may guarantee thermal acceptability. In higher temperatures cooling is needed. Below 19.5 ^{0}C the use of personal control heaters can be used. The work of the authors also considered the thermal sensation of men and women. Women are more sensitive to temperature (mainly cool) and less sensitive to humidity than men and feel more uncomfortable and dissatisfied compared to males. Women have a lower skin temperature than men. Men prefer a slightly cooler environment and women prefer slightly warmer condition. These differences in thermal sensation could be attributed to the characteristics of the metabolism and the skin surface of each gender. The review did not show any significant correlation between age and thermal comfort.

Taleghani et al [7] reviewed the development of the idea of human thermal comfort by using the steady- state model and the adaptive model. The suggested aims for thermal comfort:

- Control over indoor environment by people.
- Improving indoor air quality.
- Achieving energy savings.
- Reducing the harm on the environment by reducing CO_2 production.
- Affecting the work efficiency of the building occupants.
- Reasonable recommendation for improving or changing standards.

The paper discussed the thermal comfort in naturally ventilated buildings and centrally conditioned buildings. The relationship between comfort temperature and outdoor temperature in naturally ventilated buildings was found to be linear.

The study showed that the occupants' thermal responses in free running spaces depend largely on the outdoor temperature (and may differ from thermal responses in centrally conditioned buildings).

This is due to the different thermal experiences, changes in clothing, availability of control, and shifts in occupant expectations. The authors proposed the following equation for determining the acceptable thermal conditions in naturally conditioned spaces. These spaces must be equipped with operable windows and have no mechanical cooling system.

$T_{co} = 0.31\ T_{ref} + 17.8\ ^{0}C$ (2.1)

where

T_{ref} = prevailing mean outdoor air temperature

T_{co} = indoor comfort temperature

This equation is used for summer when the outdoor temperatures range from5 ^{0}C to32 ^{0}C, but it appears that it could be used for Khartoum, as shown in Table 2.1.

Table 2.1: Indoor comfort temperature in Khartoum.

Month	Dec	Nov	Oct	Sep	Aug	Jul	Jun	May	Apr	Mar	Feb	Jan
Max(°C)	32	35	39	39	38	39	41	42	40	37	33	31
T_{co} (°C)	28	29	30	30	30	30	31	31	30	29	28	27

Modern architecture tends to increase the window to wall ratio for aesthetic purposes and lighting. Thus solar radiation plays a main role in influencing the thermal environment around the human body. Meanwhile, given the concerns on energy saving and low carbon, people can use the solar energy for a comfortable

indoor environment, in cold climates. With appropriate energy efficient building design, the thermal comfort can be achieved with minimum electricity consumption. Our approach in this work is to improve the performance of windows, to transmit the light and reflect the heat.

Mao et al [8] offered a numerical method to analyze the dynamic thermal status of a clothed human body under different solar radiation incidences. Their method can be used to analyze the thermal status of clothed human body, under different solar radiation incidences, indoors and thus enables the architect to efficiently utilize the solar energy in building development.

2.3 Outdoor thermal comfort

Martinelli et al [9] studied the outdoor thermal comfort. They assessed the influence of daily shadings pattern on human thermal comfort. Their main findings highlighted the importance of considering daily shading pattern when renovating open spaces.

The energy balance of the human body is controlled by four meteorological variables: air temperature, water vapor pressure, air velocity and mean radiant temperature. The mean radiant temperature parameterizes the impact of all short and long wave radiation fluxes on human body. During day time, it represents the most important variable influencing human thermal comfort and it is strongly related to solar access. When solar access is restrained, as in shaded areas, direct short wave radiation fluxes are reduced and the temperature of shaded surfaces decreases; thus, long-wave radiation fluxes from the surface decline as well, producing a general cooling effect. From the physiological point of view, human thermal comforts is reached when heat flows to and from the human body are balanced and skin temperature and sweat rate are within a comfort range.

Salataetal[10] examined six different scenarios, considering the campus of the Sapienza University of Rome:

Case A: present configuration of the site.

Case B: the asphalt is replaced by a concrete pavement with a higher albedo coefficient and a lower thermal capacity.

Case C: the configuration is characterized by a roof albedo of 0.66, which are 0.31 units higher than that of the present configuration. The choice to evaluate this solution is due to the increasing interest towards cool roofs.

Case D: this configuration has a wider urban vegetation area, about 9% with respect to the present configuration.

Case E: this is a combination of the three previous mitigation.

Case F: the last configuration is not characterized by mitigation strategies of the microclimate (all the vegetation is removed) and it is assumed a ground surface made of asphalt only.

Taking as a reference point Case A (present configuration of the site), the authors noticed an improvement of the thermo hygrometric conditions in Case D and E and, as expected, a deterioration in Case F.

The effect of the cool roof (Case C) was not significant due to the distance between roofs' top and the human height level. The height of the buildings in the campus was 15 m (it sometimes reaches25 m).

Street trees can reduce high urban temperature through shading and transpiration. Coutts [11] explored the role of street trees in Melbourne in cooling the urban micro climate and improving human thermal comfort. Their results showed that street trees supported average daytime cooling by around 0.2 to 0.6 °C and up to 0.9 °C during midmorning (9:00–10:00).

Chapter Three

Smart Windows

3.1 Introduction

Smart glass is a glazing whose light transmission properties are altered when voltage, light or heat is applied [12]. Generally, the glass changes from translucent to transparent, changing from blocking some (or all) wavelengths of light to letting light pass through. Smart glass technologies include electrochromic and thermochromic.

The convergence of the architectural trend towards more use of glass (including growing interest in day lighting) and increasing demand for reducing energy use creates a unique opportunity for smart windows.

The value of variable light transmission/ absorption can best be understood in the overall context of heat and energy transfer though glazing systems. A single pane of conventional clear window glass transmits a large fraction of the solar spectrum and absorbs (but does not reflect) a large fraction of long wave infrared radiation, tending to let solar radiation in while retaining some of the black body infrared radiation emitted from surfaces inside the building (helpful in the heating season, but adds to air-conditioning loads).

However, a single glazing transfers a maximum of heat via convection/conduction (maximizing cooling season heat gain and heating season heat loss). Almost all windows include two or more panes of glass to reduce conduction/ convection.

Variable transmission glazing with suitable controls enables the best combination of day lighting levels and of minimum solar heat gain (when cooling, or maximum solar heat gain when heating), for an overall minimization of energy consumption.
When applied to the outer glazing of multiple glazing, little difference exists between reflection and absorption in the energy impact on the inside space, because the outer glazing is more closely thermally coupled to the outside air than to the air inside the building. Energy absorbed as heat in the outer glazing is primarily transferred to the outside air. This description oversimplifies many aspects of the energy performance.
Electrochromic (EC) glass and smart windows are generic terms that encompass discrete technologies that modify glass in different ways. This category includes approaches such as liquid crystal systems that change from clear to translucent and photochromic glass that darkens in sunlight.

3.2 Electrochromic Windows

Smart window technology based on electrochromic (EC) glass is entering early commercialization and has significant implications for the future design and outfitting of commercial and residential buildings. Metal oxide electrocromics technology consists of a five-layer metal oxide coating sandwiched between two sheets of glass [12].The layers are: conductive layer, positive ion storage layer-colorless lithium metal oxide, conductor/electrolyte layer, electrochromatic layer-negative tungsten oxide, and conductive layer.
All of the layers are applied by vacuum deposition (sputtering). When voltage is applied, lithium ions travel from the positive layer through the conductor/ electrolyte layer and into the electrochromatic layer to react with tungsten oxide to form lithium tungstate. As this occurs, a charge-compensating electron flows

through the circuit from the ion storage layer to the electrochromatic layer. Lithium tungstate is light absorbing and as the reaction proceeds, the glass darkens and sunlight is absorbed within the glass as heat.

Reversing the polarity causes the reaction to be reversed and the glass reverts to its clear state. The range of typical products is from 62% visible light transmission when clear to 3.5% transmission in the fully tinted state.

Glass of this composition provided by the leading developer is typically fabricated into industry standard insulating units (IGUs) and installed in frames supplied by the developer, its partners or independent suppliers. The IGUs are operated by a control system, which can range from manual adjustment of a single window to a whole-building automation system. The electricity needed to power and control 140 m^2 of glass (approx. 100 windows) is less per day than a single 60 W light bulb, and no power is consumed at all when the glass is kept in the fully clear state [12].

Metal oxide electrochromic glass was developed with funding from federal government grants and has benefited from testing by several government laboratories. Indications are that electrochromic glass of this type has good durability and can be cycled from clear to tinted more than 100,000 times without loss of functionality. In a cooling-dominated environment, smart windows significantly reduce heat gain and the energy demands of cooling. Lighting costs also are reduced under all conditions.

A performance characteristic of this electrochromic glass that may limit its broad adoption is switching speed. The transition from clear to opaque takes three to five minutes for a small window and the darkening proceeds from the edges to the center of the glass over that period of time [12]. Larger windows and/or lower temperatures take longer. Because of the time needed to tint the glass, the standard use is to control the system for just two states: clear and fully tinted.

In the future, intermediate levels of tinting may be offered. However, fast responses to such short term changes as clouds moving over the sun are not possible with this technology and user (or control system) real-time fine-tuning of the amount of light entering the room is limited by the long delay in the response of the window.

During the winter the heat is needed inside the buildings, and at the same time the light is needed to be transmitted throw the windows. In the summer time, the window is required to transmit the light and reflect the heat. Electrochromic devices change light transmission properties in response to voltage and thus allow control over the amount of light and heat passing through. It changes between a colored, translucent state (usually blue) and a transparent state. A burst of electricity is required for changing its opacity, but once the change has been achieved, no electricity is needed for maintaining the particular shade which has been reached.

Electrochromic glass provides visibility even in the darkened state and thus preserves visible contact with the outside environment. Hong and Chen [13] used Nano-Prussian blue analogue/PEDOT/PSS: composites for a 10 x 10 cm^2WO_3electrochromic window. A maximum transmittance modulation of 61.6% at a voltage of 1.6 V was obtained. Kim and Taya [14] used V_2 O_5 and poly (3, 3-dimethyl-3, 4-dihydro-2H-thieno [3,4-b][1,4]dioxepine) coatings. The window demonstrated electrochemical stability after over 150,000 cyclic switches, and that the response time for a 25 x 25 mm^2 window was 5 seconds for coloration and 4 seconds for bleaching. Similarly, Kim et al [15] obtained high electrometric contrast and optical cyclic stability, when they used electrochromic windows based on anodic electrochromic polymesitylenes containing 9H-carbazole-9-ethanol moieties. Fernandes et al [16] used

glass /ITO/WO_3/ electrolyte /ITO/ glass layered configuration. That resulted on visible average transmittance variation and optical density change of 41.6% and 0.39, respectively. Hee et al [17] concluded that electrochromic windows are more suitable for applications in residential areas in cold climate regions. Brooke et al [18] investigated the effect of oxidant on the performance of conductive polymer films. They concluded that the oxidant Fe $(Tos)_3$ produced superior device performance with respect to optical switching, switch speed and optical relaxation. Kim et al [19] prepared transparent conductive ZnInSnO-Ag- ZnInSnO multilayer films for polymer dispersed liquid- crystal based smart windows. They obtained a lower operating voltage and a higher cutoff rate of infrared light, compared to ITO or ZITO-based smart windows. Khandelwal et al [20] fabricated electrically switchable broadband infrared reflectors using polymer stabilized cholesteric liquid crystals. They predicted that their reflector can save more than 12% of energy compared to double glazing window and 9.3% compared to static infrared reflector. One of the drawbacks of electrochromic windows is their need for external biases to operate. Wang et al [21] introduced a self-powered window. Aluminum was used to reduce Prussian blue to Prussian white in potassium chloride electrolyte. For self-recovering of the device to the blue appearance, the aluminum and Prussian blue electrodes could be disconnected. Lim et al [22] studied the performance of tungsten-oxide-based electrochromic window. The results showed that the transmittance of visible light varied from 64% in the clear state to very low values in the colored state. They also concluded that there is little additional benefit from placing low emissivity coating on the electrochromic window. Ranjit A. Patil et al [23] used pure1DbrookiteTiO_2nanoneedles grown on a conducting indium tin oxide thin film coated glass substrate. The electrochromic characteristics include stable and reversible coloration–bleaching cycles, and high-value diffusion coefficient (1.56×10-11cm^2/s), high reversibility(~99%), great

coloration efficiency (226cm^2/C), high optical transmittance difference (67%), large optical density(0.85), and fast coloration and bleaching times (13.10and5.14s) at a wavelength of 600nm.

3.3Thermochromic windows

Thermochromic windows switch from a clear state in low temperature to a diffuse reflective state in high temperature [24].The results of Linshuang Long et al [25] showed that the adoption of the VO_2 double-glazed window reduced the cumulative cooling energy consumption by approximately11.1% compared with an ordinary double-glazed window. Zheng et al [26] designed TiO_2(R)/VO_2 (M)/TiO_2 (A) multilayer film to work as a smart window with antifogging and self-cleaning functions. Koo et al [27] fabricated CeO_2 –VO_2bilayer to improve the optical properties of VO_2 window. The CeO_2 was employed as an antireflection layer of the VO_2film.Kamalisarvestani et al [28] studied the spectral selective properties of thermochromic windows and the effect of doping of VO_2 coatings with different dopants.

VO_2 could be the most promising thermochromic material, but its drawback is the preparation cost and the stability. Polymer-assisted deposition preparation method could be more suitable for practical applications than gas-phased methods [29]. Another promising technology is a multilayer thin film structure, consisting of dielectric and metal layers [30]. Batista et al [31] concluded that tungsten was the most effective dopant on the reduction of the semiconductor-metal transition temperature of VO_2. More energy could be saved by using VO_2 double window. Long and Ye [32] suggested that an appropriate phase transition temperature is needed to make the VO_2 remains principally in its metallic state with low solar transmittance for summer application and in its semiconductor state with high solar transmittance for winter application. Zhou et al [33] combined a

VO_2thermochromic window with solar cells operated by the scattered radiation from the window. However, the efficiency of the cell was too low to justify the additional cost. Wei Feng et al [34] studied the effect of Gasochromic (GC) smart window on the energy consumption for a commercial office building. The results showed that GC smart windows can decrease the annual consumption of heating, ventilation and air condition (HVAC) loads by 25–35% in all cities.

Both electrochromic and thermochromic windows suffer from high cost, low transmission of visible light and slow response time. In tropical regions, the ideal window is the one which transmits all the visible light to reduce the lighting load, and reflects all the infrared radiation to reduce the cooling load. In the following chapters, we develop a relatively cheap and simple filter which suits the conditions of Sudan.

Chapter Four

Simulation

4.1 Introduction

Simulation is the process of designing a model of a real system and conducting experiments with this model for the purpose either of understanding the behavior of the system or of evaluating various strategies (within the limits imposed by a criterion or set of criteria).The simulation is used in this work for designing a filter, to be used in hot climates. The filter consists of ITO and four periodic pairs of Si/SiO_2, deposited on a glass sheet. Similar approach has been used successfully, before, for designing and testing a filter for a thermo photovoltaic system [35].The simulation was based on rigorous coupled-wave analysis (RCWA) method.

4.2 Rigorous coupled-wave analysis

(RCWA) is formulated in the 1980s by Moharam and Gaylord. It is used for analyzing the diffraction of electromagnetic waves by periodic gratings [36]. RCWA is used in this study to calculate the radiative properties (reflectance and transmittance) of the periodically multilayer surfaces. It analyzes the general diffraction problem by solving Maxwell's equations accurately in each of the three regions (input, multilayer, and output), based on Fourier expansion [37]. In RCWA, diffraction efficiency for each diffraction order is calculated with incident wave properties regardless of feature size, structural profiles, and dielectric function of the materials.

The dielectric function of the materials is expressed as, $\varepsilon = (n + ik)^2$ where n is the refractive index and k is the extinction coefficient. The accuracy of the solution

computed depends solely upon the number of terms retained in space harmonic expansion of electromagnetic fields, which corresponds to the diffraction order. Any linearly- polarized incidence can be decomposed into the transverse electric (TE) and transverse magnetic (TM) mode. The normalized electric field of incidence E_{inc} can be expressed as:

$$E_{inc} = \exp\left(ik_x x + ik_z z - iwt\right) \tag{4.1}$$

The electric field in region I (Fig.3.1) is the superposition of the incident wave and the reflected waves; therefore

$$E_1\left(x,z\right) = \exp\left(ik_x x + ik_z z\right) + \sum_j E_{rj} \exp\left(ik_{xj} x - ik_{zj}^r z\right) \tag{4.2}$$

Similarly, the electric field in region II (E_{II}) is the a superposition of all transmitted waves

$$E_{11}\left(x,z\right) = \sum_j E_{tj} \exp\left(ik_{xj} x - ik_{zj}^t z\right) \tag{4.3}$$

The magnetic field in region I and II can be obtained from Maxwell's equation H

$$H_I\left(x,z\right) = -\frac{i}{\omega\mu_0}\left(\nabla \times E_I\right) \tag{4.4}$$

$$H_{II}\left(x,z\right) = -\frac{i}{\omega\mu_0}\left(\nabla \times E_{II}\right) \tag{4.5}$$

where ω represents the frequency and μ_0 the magnetic permeability of vacuum. The electric and magnetic field components in region M can be expressed as a Fourier series:

$$E_M\left(x,z\right) = \sum \chi_{yj}\left(z\right) \exp\left(ik_{xj} x\right) y \tag{4.6}$$

$$H_M(x,z) = \frac{ik}{\omega\mu_0}\sum_j \left[\gamma_{xj}(z)\,x + \gamma_{zj}(z)\,z\right]\exp\left(ik_{xj}x\right) \qquad (4.7)$$

where χ_{yj} and γ_{xj} are vector components for the jth space-harmonic electric and magnetic field in region M (multilayer region), respectively. Due to the structure periodicity, the relative dielectric function in region M, $\varepsilon(x)$ and its inverse $\frac{1}{\varepsilon(x)}$, can also be expanded in Fourier series:

$$\varepsilon(x) = \sum_p \varepsilon_p^{ord} \exp\left(i\frac{2p\pi}{\Lambda}x\right) \qquad (4.8)$$

$$\frac{1}{\varepsilon(x)} = \sum_p \varepsilon_p^{inv} \exp\left(i\frac{2p\pi}{\Lambda}x\right) \qquad (4.9)$$

where ε_p^{ord} and ε_p^{inv} are the jth Fourier coefficient for the ordinary and inverse of $\varepsilon(x)$,respectively.

4.3 Result

4.3.1 Optimization of Si Thickness

The glazing consists of ITO layer deposited on one-dimensional (ID) four pairs of Si/SiO_2 layers on top of a 1mm-glass sheet, Fig.4.1. The geometric parameters used to illustrate the wavelength selective filter are the thicknesses of the layers. The wavelength-dependent dielectric optical constants of ITO, silicon and silicon dioxide were obtained from Ref [38]. The thickness of ITO was 0.1μm and that of Si was d_1=0.1, 1.5 and 0.2μm. The thickness of SiO_2 was fixed at d_2=0.4μm.The normal reflectance and transmittance for the proposed selective filter were calculated numerically by using RCWA method in the wavelength

range from 0.3 μmto3 μm. The normal reflectance and transmittance of the glazing, at normal incidence TM waves, is shown in Fig.4.2.The results show that the optimum thickness of the Si is 0.15μm. It gives low reflectance (lessthan30%) for wavelengths less than 0.8μm and reflectance of nearly unity for higher wavelength values. This would transmit most of the visible light (to reduce the lighting load) and reflects nearly all the infrared (to reduce the cooling load).

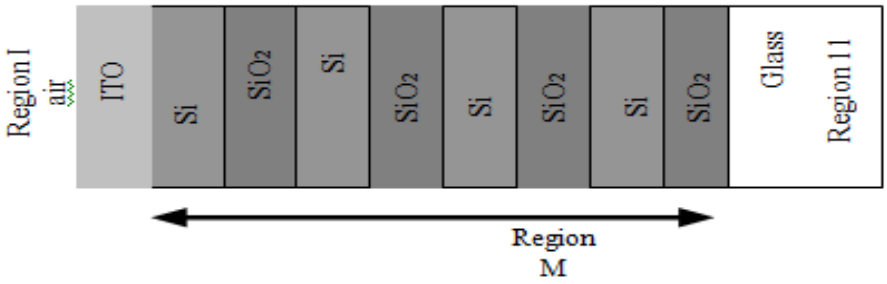

Figure4.1Selective filter components.

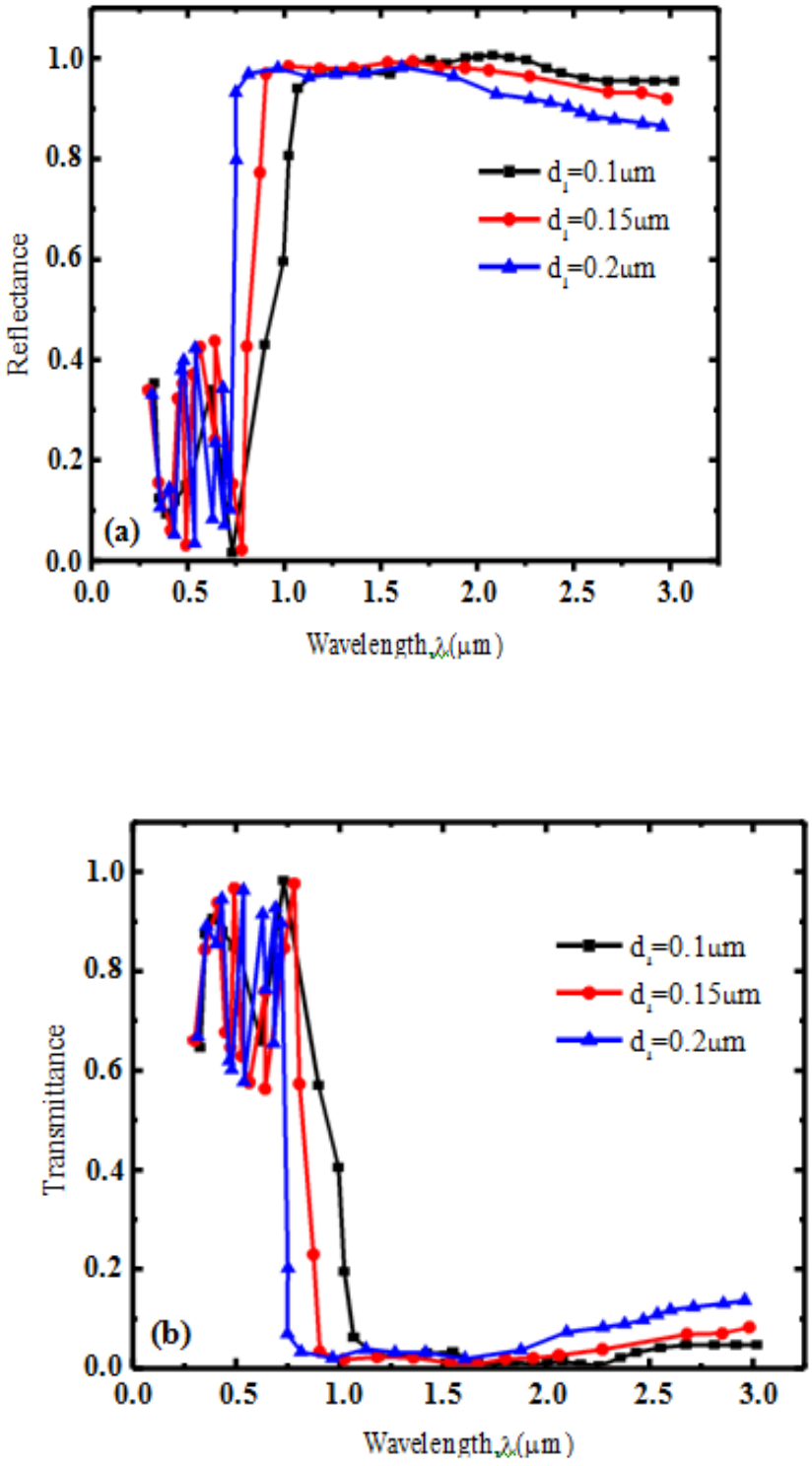

Figure.4.2 The proposed selective filter for wave with different $d_1$thicknesses (a) shows the reflectance and (b) the transmittance.

4.3.2 Optimization of SiO_2 Thickness

Figure.4.3 shows the normal reflectance and transmittance of the glazing for normal incidence TM waves. The thickness of Si was fixed at its optimum value (0.15μm), while that of SiO_2 was changed, d_2 = (0.2, 0.3 and 0.4) μm. The results show that the optimum thickness for $SiO_2$is 0.4μ*m*. The figure shows that when the sickness of Si is chosen to be 0.15μm and that of SiO_2 to be0.4μm, the filter transmits 70-80% of the visible light and reflects almost all the infrared radiation.

The glazing not only reduces the electricity consumption during daytime, but it also acts as an insulator during the cold nights of winter. It reflects the heat back inside the room. In the desert, the air temperature drops to less than10^0C during the night. When the room temperature is about 30^0C, which corresponds to a peak wave length of about10μm, there would be very little heat loss through the windows, Figure.4.4.

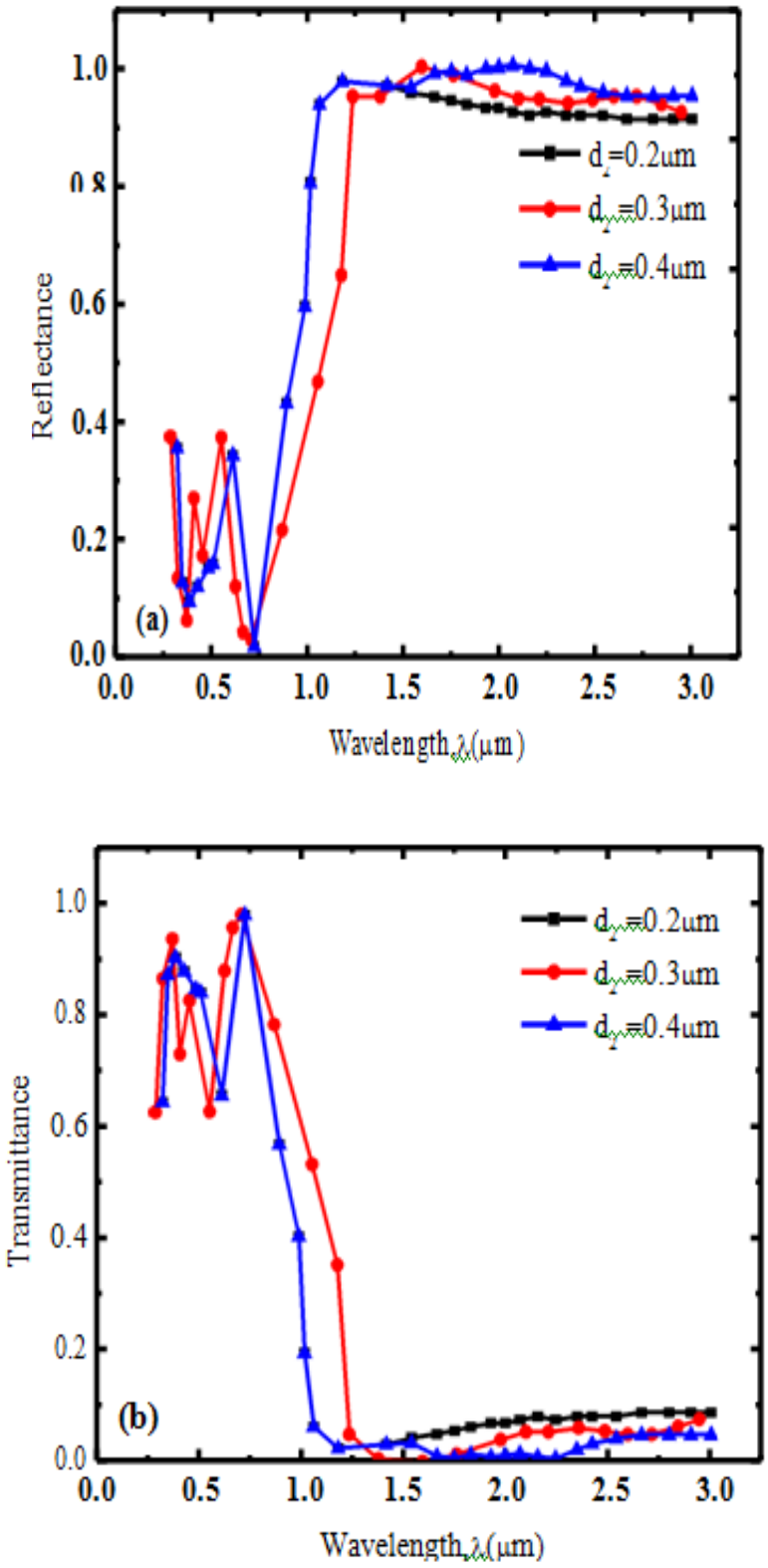

Figure.4.3 the glazing with different SiO_2thicknesses.(a)shows the reflectance and(b)the transmittance.

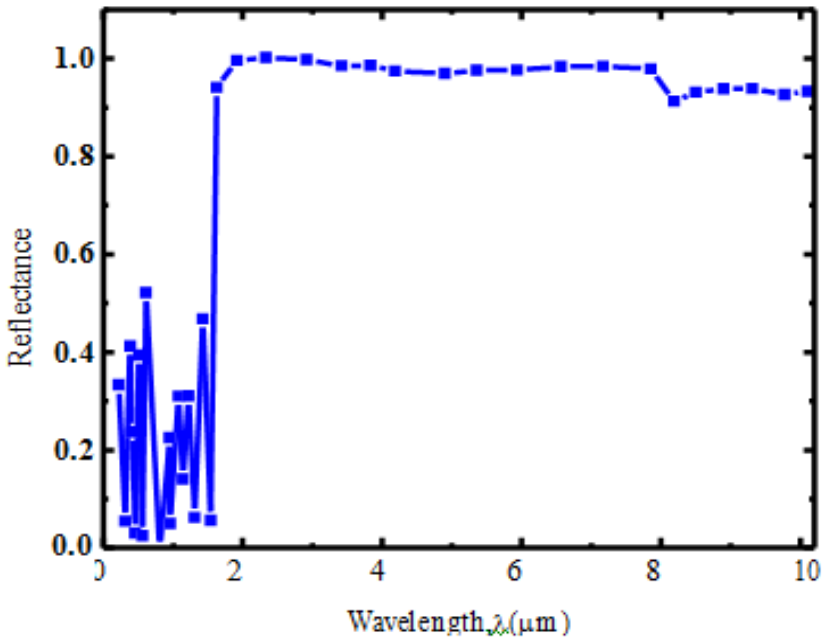

Figure.4.4: The optical properties of the glazing in the infrared range makes it a potential insulator during the cold nights.

4.3.3 Effect of incidence angles

The effect of the angle of incidence on the reflectance and transmittance is shown in Figure.4.5 It is seen that increasing the angle of incidence from 0^0 to 60^0 makes little difference on the reflectance and transmittance. The glazing seems to be suitable for all seasons and for both direct and diffuse radiation.

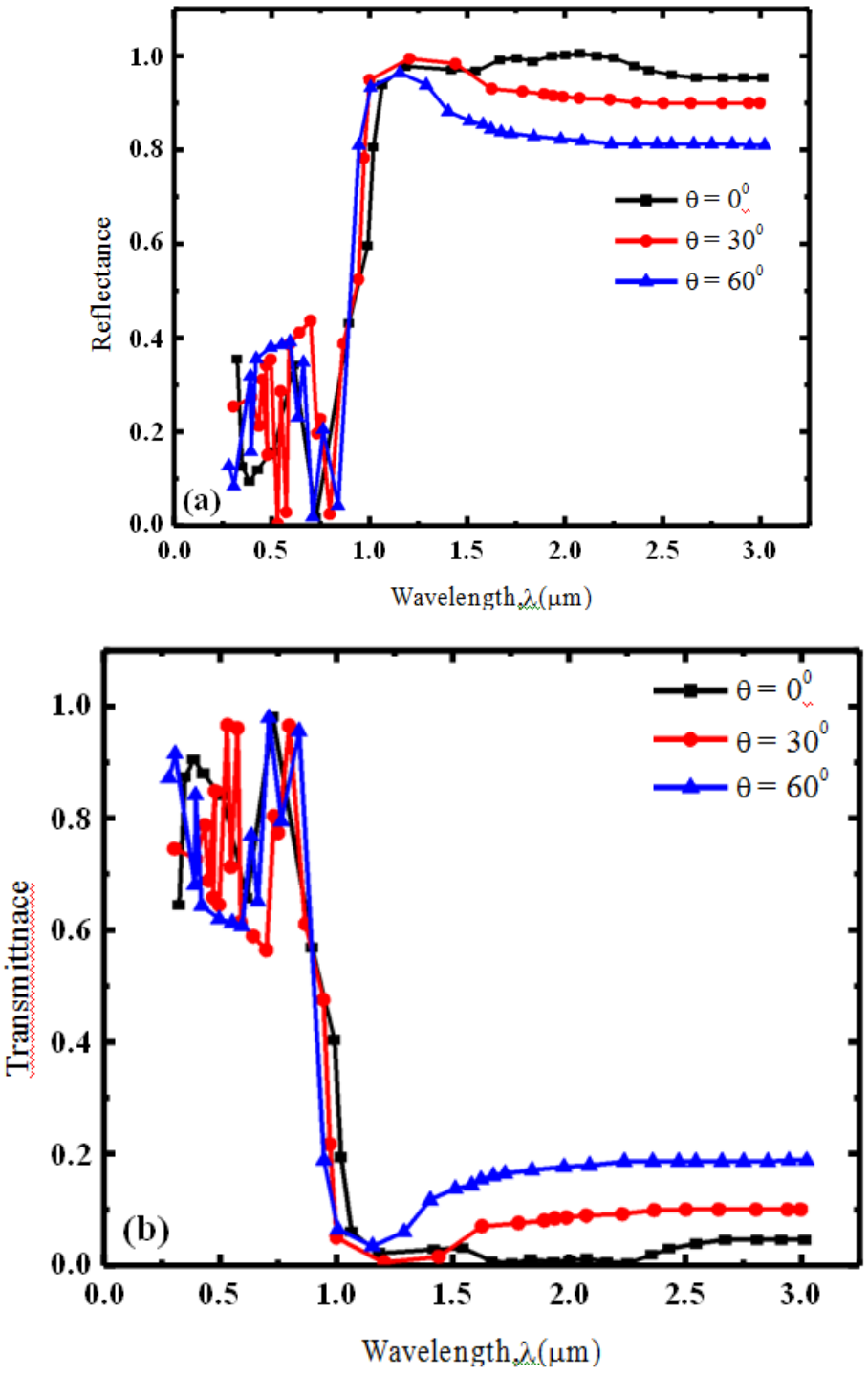

Figure.4.5:The performance of the glazing for different incidence angles. (a) reflectance and (b) transmittance.

4.4 Summary

The results of the simulation show that the optimum thicknesses of ITO, Si and SiO_2 were 0.1, 0.15ando.4μm, respective. The glazing acted as an optically selective filter. It transmitted 70-80% of the visible light and reflected almost all the infrared radiation from the sun. The optical properties of the glazing hardly depend on the angle of incidence of solar radiation. This makes it ideal for all hours of the day. During the night, in winter, it could act as an insulator to reflect the heat back inside the room. It satisfies the conditions for comfort in both the hot days of summer and the cold nights of winter.

Chapter 5

Instrumentations

5.1 Introduction

In this chapter, the instrumentations for preparing and measuring the thicknesses of the different layers of (Si/SiO_2) and the performance of the filter, are described. Periodical multilayer microstructures selective filter was produced by magnetron sputtering technique. The spectrophotometer was used to measure the reflection and transmission of the radiation.

5.2 Magnetron Sputtering Subsystem

The system employs sputter deposition which is often commonly referred to as sputtering. Sputtering is a process whereby atoms of a solid target are ejected (or vaporized) due to the 'momentum transfer from an atomic-sized energetic bombarding particle' impinging on the target surface [39]. These vaporized particles will then condense upon and coat a substrate material. Typically sputtering is performed using gaseous ions from plasma that are then accelerated and directed toward the target (although it is also possible to use an ion gun in place of generating ions by producing plasma). The system uses plasma produced and controlled by magnetron guns. The magnetron sputtering system provides the solid material to be deposited onto the substrate. Sputtering is the physical vaporization of atoms from a target surface to form a thin film onto a substrate by momentum transfer from bombarding energetic atomic sized particles. These atoms, ejected from a target, have a wide energy distribution. The vacuum chamber

of the physical vapor deposition (PVD) is filled with an inert gas such as argon. The advantages of the magnetron sputtering that it uses magnets to increase the percentage of electrons that take part in ionization events, increases probability of electrons striking argon, increases electron path length, lowers voltage needed to strike plasma, controls uniformity, reduces wafer heating from electron bombardment and increases deposition rate. There are large varieties of techniques for sputter deposition of the materials such as radio frequency (RF) magnetron sputtering, DC magnetron sputtering, pulsed DC magnetron sputtering, ion and plasma beam sputtering[39]. Figure 5.1 shows the magnetron sputtering system which has been used in this work at the laboratories of the Faculty of Science, University of Witwatersrand, South Africa.

Figure. 5.1: The sputter deposition system

5.2.1 Magnetron Sputtering Guns and Target Configuration

The geometry of the sputter deposition system determines many of the factors that affect the properties of the deposited film and the throughput of the system [39]. Yet there are also more obvious practical design considerations that are determined by the use of a sputter system. Sputtering allows for the overall system to be much more compact and for the target to substrate distance to be smaller. This is because the sputter sources operate at lower temperatures and cause less heating than would be found in a vaporization based system [39]. A smaller volume system will have less space to be evacuated and less surface area for contaminants to adsorb onto. This decreases pump down time and makes it easier to maintain high system

purity. A magnetron sputter system also provides for co-deposition of films by using multiple magnetron guns spaced closely together. The three magnetron guns used in this work are shown in Figure 5.2. The arrangement approximates a cylindrical target and allows a more uniform distribution of incident flux on an object placed at the center or focus of the slightly angled magnetron guns. The vertical position of the sample can be adjusted so that it is at the focus of the three guns. Each magnetron has its own shutter so that it can be protected from sputtered material when not in use.

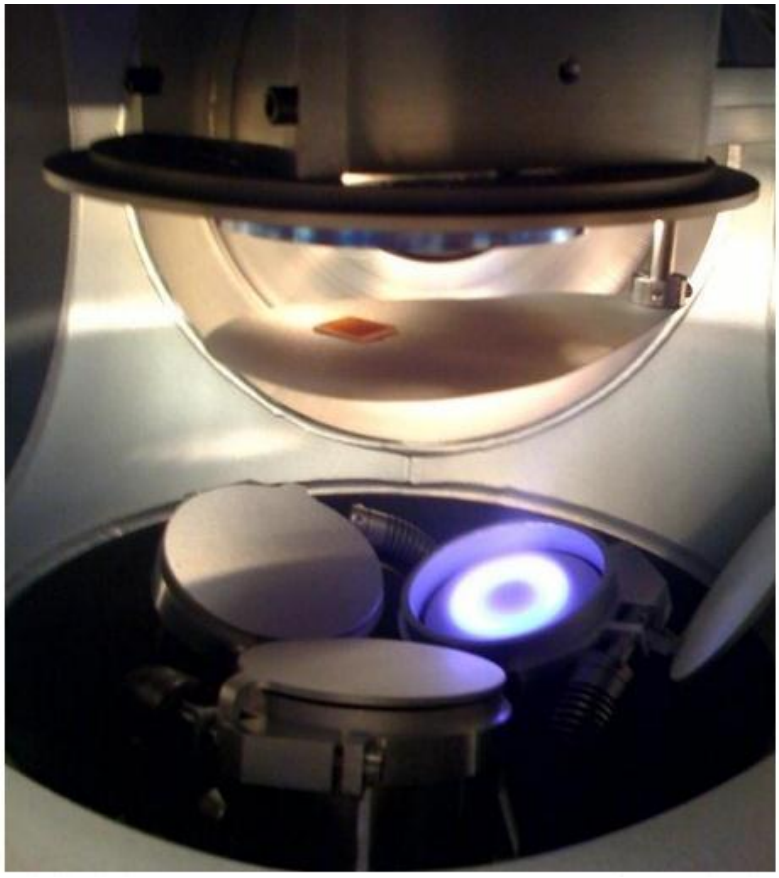

Figure 5.2: Active argon plasma and substrate heater as seen from main viewport

5.2.2 Sputter Targets

The targets themselves are simply 3-inch (diameter) disks of the chosen material. Sputter targets are ‘‘long-lived sources’’ ideal for two-chamber PVD systems where the main chamber should be open to the ambient as infrequently as possible for maintenance [39]. The targets used in the system are minimum ‘‘three nines’’ purity (or 99.9% pure). To prevent overheating (and melting) of the targets the magnetron guns are actively cooled. To increase heat removal, the targets are typically screwed or bonded to a copper backing place. The uranium and cerium targets are both brittle causing the threads to break off thus detaching the targets from the copper plates un lessbonded with thermal compound. Alternatively, if the guns are operated at a low enough power, the targets can be placed in the guns without a backing plate. However, the choice of power supply can also affect this decision. For example, RF power supplies can cause non-conducting materials to heat rapidly. Heating of the targets can cause them to expand slightly, but the greatest change in the target shape is from sputtering. In planar magnetron sputtering the target develops a ‘racetrack’ depression on the surface. This changing geometry can affect the deposition rate, vapor flux distribution, and other deposition parameters such as the amount of reactive gas needed for reactive deposition in reactive sputter deposition. Typically, only a fraction of the sputter target (usually 10 to 30 percent) is used as the “racetrack erosion’’ determines the overall lifetime of the target [39]. This time can be increased by removing the target and melting it so that the surface becomes uniform once more. However, this can introduce impurities into the target and it is usually simpler and more cost effective to buy a new target.

Another consequence of sputtering the target is that they may become coated in a thin smut of fine particles. These particles may result from poisoning of the target, gas-phase nucleation, or ‘‘cross-talk’’ with other sputter guns (where there material is deposited on another nearby target). These particles can be simply wiped off during maintenance or can be cleaned in system using ‘‘pre-sputtering’’ [39]. Pre-sputtering is simply sputtering of the target for a given length of time while the substrate is shielded by a shutter or held in the load-lock chamber. Sputtering removes adsorbed contaminants from the surface of the target and is most commonly used to remove any excess compound created by the reactive gas. It is important to note that the surface morphology of a sputter target can affect the morphology of a sputter deposited film. A smooth, clean sputter target will produce a more uniform flux of sputtered atoms. Therefore the target should always be pre-sputtered before film fabrication and for an increased time after system maintenance that involves opening the main chamber.

5.2.3 Power Supplies

The magnetron guns can be powered by either a DC power supply or a RF power supply. The power supplies used have built in readouts and can be controlled by means of the voltage, current and/or total power. The RF matching network for the RF power supply is a separate component located on the system support frame and requires the use of a copper grounding strip. The DC supplies have built-in arc suppression circuitry.

There are currently a total of three power supplies; two DC power supplies and one RF power supply. This allows for all three guns to be operated simultaneously or for two guns to be operated while a voltage bias is applied to the sample holder (and substrate). Each type of power supply has its own advantages and

disadvantages. RF power supplies are more complex than DC supplies and require the use of an impedance matching network to maintain a constant net voltage. (By net voltage it is meant to mean the average voltage at which the RF signal oscillates above and below.) RF power can also ‘‘creep’’ along metal surface and can present a hazard unless the system is properly grounded. Nevertheless, there are distinct advantages to RF supplies. RF can be used to activate plasma at pressure lower than 1 mTorr (given the right geometry and gas flow). (This is lower than what DC supplies are generally capable of because there plasma may be less dense for a given power level.) This reduces the chances of ‘‘poisoning the target’’ with too much reactive gas or of causing arc formation on the surface of the target. (Arcing can damage the magnetron guns and most supplies are built with arc suppression circuitry.) Finally, although this is not currently a feature, both an RF and DC potential can be applied to a single target (as long as there is a RF choke in the DC circuit to prevent damage of the power supply) [39].

5.2.4 Quartz Crystal Monitor

Finally, there must be a means of determining the amount of material sputtered from the target and deposited onto the substrate. To do this the deposition time is recorded and the deposition rate is measured using a quartz crystal deposition monitor or QCM for short. A QCM is a real-time in situmonitor that functions by applying a voltage at a high frequency (usually around 5 MHz) to a piece of single crystal quartz. Because the quartz is a piezoelectric material, the applied voltage causes the volume of the crystal to increase. Since the voltage is applied at a high frequency the crystal resonates with a frequency that is determined by the magnitude of the voltage, and the crystal properties. As material deposits on the quartz, the resonance frequency decreases proportionally to the amount of mass added. It is this frequency change that is used to determine the amount of film

deposited onto the QCM and, indirectly, the amount deposited onto the substrate. [39] .In order to approximate the film deposited onto the substrate the QCM must be calibrated. First, the density of the material deposited must be input into the QCM controller then the z-factor must be entered. The z-factor is the ratio of acoustical impedance of the film material to that of the quartz crystal. (Again, crystal properties such as its crystalline orientation affect this value.) It should also be noted that heating of the QCM due to high deposition rates may affect the resonance and artificially alter the deposition rate. This can be accounted for by applying coolant to the QCM (which is an optional feature of the system). Another factor which may affect QCM accuracy is film stress of the film on the crystal. (This effect can only be calculated by comparing the deposition rate to a different QCM with a different crystal orientation.)

Finally, a tooling factor must be determined experimentally that correlates the amount of material deposited on the QCM with the amount on the substrate for a given time. (The amount of material will be calculated by the QCM controller and the amount on the substrate will have to be determined using one of the techniques described. The resulting ratio is then the tooling factor.) The tooling factor for the system will most likely be greater than one as the amount of material deposited on the substrate will most likely be several times greater than that deposited on the QCM. This is by design. The QCM was positioned off-axis and at an angle with respect to the sputter gun so as to reduce the material deposited on the crystal. This increases the lifetime of the crystal because after a certain amount of material has been deposited on it the crystal needs to be replaced. It is also important to note that the tooling factor will vary depending on which gun is used to deposit the material (as the angle is different with respect to the QCM is different for each).

When co-depositing material the results of the QCM will be less accurate. The only way to account for this would be to add more QCMs to different locations in

the chamber or to use an alternative method of deposition rate monitoring. Other methods researched included ionization deposition rate monitors and optical adsorption spectrometry based monitors. Both of which would require altering the system geometry and would be calibrated only for the particular depositing material (and a fixed geometry). These costly alternatives were eliminated and only a single QCM system was implemented. The use of a single QCM greatly simplifies the overall system design while still allowing the approximate amount of material deposited to be determined during sputtering. All samples produced in the system will be characterized fully; this includes the depth profile of each sample to determine the final, exact thickness.

5.3 Gas Distribution System

The gas distribution system consists of a (vacuum) chamber, a pump for evacuating (or reducing the pressure of) the chamber, a means of measuring and introducing gas into the system, and a means of measuring and controlling the overall pressure in the chamber. The basic design decisions involved in developing the gas distribution system will be detailed in this section.

5.3.1 Pumping System Design

The level of cleanliness desired for a particular process determines the vacuum range at which a system is required to operate. By extension it determines the type of vacuum pump or pumps required to achieve and maintain the vacuum. The lower the pressure (or higher the vacuum) required the greater the price of system components and the higher the degree of system cleaning and preparation required.

5.3.2 Pressure Measurement and Pressure Control using the Gate Valve

Several types of pressure sensors are used in this system design. These sensors function based on different methods which determine the range of operability.

5.3.3 Gas Supplies, Mass Flow Controllers, and the Gas Injection Manifold

The reactive gas and the working gas supplies used are ‘‘five nines’’ and ‘‘six nines’’ pure, respectively (i.e. 99.999% O2 and 99.9999% Ar). Each gas supply used a dual-vane high-purity all stainless steel regulator valve (specific to that gas/bottle connection). Use of dual-vane regulators, as opposed to single vane

regulators, allows the gas supplied to remain at a continuous (non-fluctuating) pressure as long as there is gas available in the tank. The regulators have stainless steel VCR connections and are connected to lock-in integral VCR valves (which were cleaned by the manufacturer to clean room standards). The secondary valves then connect to custom-ordered ¼ in. stainless steel piping with VCR connections that were bent into the desired shaped using a pipe bender. These metal gas lines transport the gases to their respective Mass Flow Controllers (MFCs). The tanks and associated valves and piping are shown in Figure 5.3. Note that for safety purposes, the O_2 line also has a flash suppressor so that if flammable gas were somehow introduced into the line and ignited it could not back flow into the O_2 tank. Additionally, the regulators only allow pressures of up to 30 to 40 psi. This is intentional so that the gas lines cannot become over-pressurized [39].

Figure 5.3: Gas tanks (left to right: O_2, Ar, “low” purity Ar, and Air) and associated hardware.

5.4 Safety and Support Systems

In addition to the Magnetron sputtering and Gas Distribution subsystems, there are many auxiliary systems required to allow these components to function normally. These systems include basics such as an adequate coolant supply as well as the foundation for more advanced safety-related features.

5.5 Maintenance and Cleaning

Regular maintenance and cleaning will need to be performed on the magnetron sputtering system. For practical and convenience purposes, it was designed to minimize down times associated with these tasks.

5.6 Sample Storage

Although not technically part of the system, there are several storage options available for completed film samples. The storage methods are designed to mitigate the post-deposition contamination of the films. Examples of post-deposition include oxidation of the completed film or the adsorption of contaminants such as hydrocarbons. (Water vapor accumulation can also be detrimental to films).While inside the system, post-deposition contamination will remain unlikely.

5.7 Scanning Electron Microscopy

A scanning electron microscope (SEM) is a type of electron microscope that uses a focused beam of high-energy electrons instead of light to generate a variety of signals at the surface of solid specimens to form an image. These signals produced by a SEM include secondary electrons, back-scattered electrons (BSE), photons characteristic X-rays, cathode luminescence (CL) and heat. The electrons which come from the electron gun are focused on the surface of the sample and some interactions occur between sample surface atoms and incoming electrons. The surface of the sample ejects electrons called (secondary electrons) then these electrons are collected by appropriate detectors and the output is modulated to give a contrasted electron image. These secondary electrons are most valuable for

showing morphology and topography of the samples. The x-y scanning modes then give a fully scanned and contrasted electron image. If the sample is a conductive metal, then there is no need for the preparation before being used and a good image quality could be obtained. The quality of the image decreases for non-metallic samples and so they should be made conductive by covering the sample with thin layers of gold. The scanning electron microscope has many advantages with respect to optical microscopes such as; a large depth of field about 30mm, much higher resolution, higher magnification and it uses electromagnets rather than lenses. The researcher has much more control on the degree of magnification. The obvious drawback of SEM is that it is very expensive, complicated, and it requires an expertise to operate it [40]. Figure 5.4 shows scanning electron microscope (SEM) system WARNING (Wits) of Technology Lab.

Figure 5.4 Scanning Electron Microscope (SEM) system, WARNING (Wits) of Technology Lab.

5.8 Spectrophotometer

Spectrophotometer is a scientific method based on the absorption of light by a substance, and takes advantage of the two laws of light absorption. Spectrophotometer is designed to measure the degree of absorption of light by a substance, in a definite and narrow wavelength range. The absorption spectrum in the visible and ultraviolet regions of a substance in a solution is characteristic depending on its chemical structure. Therefore, the spectrophotometer is used to identify a substance by measuring the absorbance at various wavelengths. This method is applicable to identification tests, purity tests, and assays, in which the absorbance of a solution with a certain concentration is usually, measured at the wavelength of the maximum absorption (λ max) or the minimum absorption (λ min). When monochromatic light passes through a substance in a solution, the ratio of the transmitted light intensity (I) to the incident light intensity (I_0) is called transmittance (T), while the common logarithm of the reciprocal of transmittance is called absorbance (A).

Spectrophotometer is a measurement of how much a chemical substance absorbs or transmits and a spectrophotometer is an instrument that measures the amount of the intensity of light absorbed after it passes through sample solution. With the spectrophotometer, the concentrations of a substance (the amount of a known chemical substance) can also be determined by measuring the intensity of light detected. It can be classified into two different types, depending on the range of wavelength of light source. The basic structure of spectrophotometers it is represented in Figure 5.5. It consists of a light source, a collimator, a monochromatic, a wavelength selector, acurette for sample solution, a photoelectric detector, and a digital display or a meter. Illustrates Figure5.6. A single wavelength spectrophotometer.

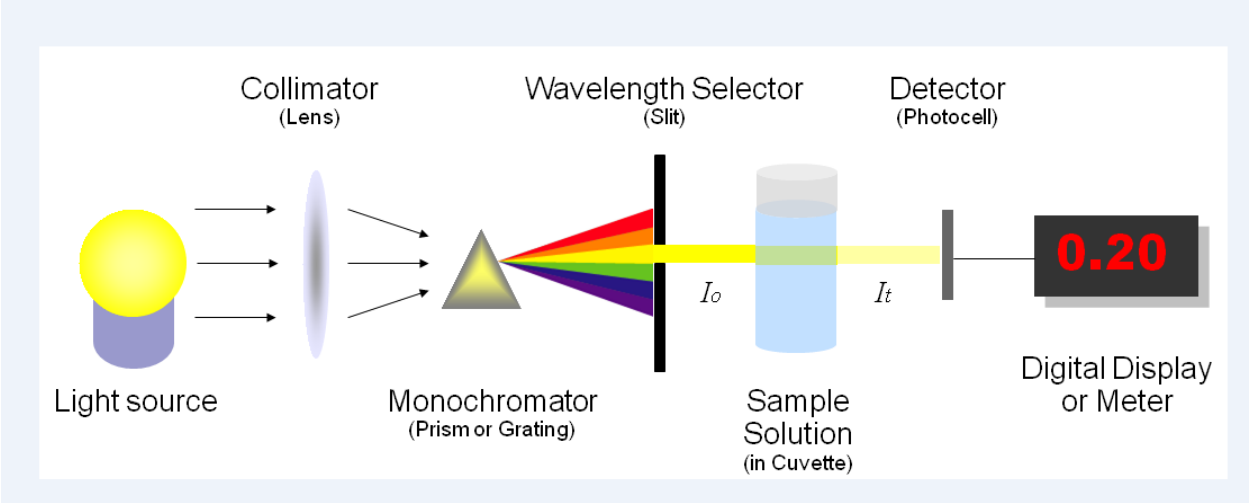

Figure 5.5: Basic structure of spectrophotometers

Figure 5.6: A single wavelength Spectrophotometer

A spectrophotometer, in general, consists of two devices; a spectrometer and a photometer. A spectrometer is a device that produces, typically disperses and measures light. A photometer indicates the photoelectric detector that measures the intensity of light. Spectrometer: It produces a desired range of wavelength of light. First a collimator (lens) transmits a straight beam of light (photons) that passes through a monochromator (prism) to split it into several component wavelengths (spectrum). Then a wavelength selector (slit) transmits only the desired wavelengths. Photometer: After the desired range of wavelength of light passes through the solution of a sample in cuvette, the photometer detects the amount of photons that is absorbed and then sends a signal to a galvanometer or a digital display [41].

Chapter Six

Experimental Setup and Fabrication

6.1 Design and construction

6.1.1 Basic Sputtering Process

The preparation of the filter and the testing were performed at the laboratories of the Faculty of Science, University of Witwatersrand (Wits), South Africa. A schematic diagram of the basic components of the sputtering system is presented in Fig 6.1.

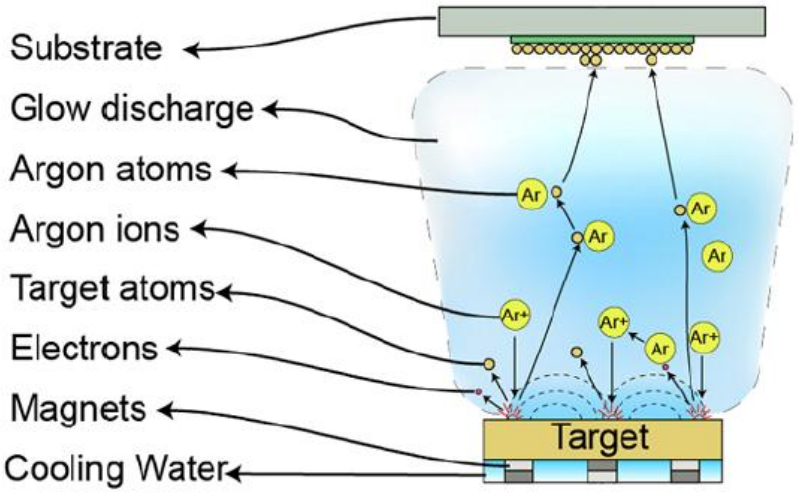

Figure 6.1: basic components of a sputtering system [1].

There are many different ways to deposit materials such as metals, ceramics, and plastics onto a surface (substrate) and to form a thin film. Among these is a process

called (sputtering) that has become one of the most common ways to fabricate thin films. Sputtering is a physical vapor deposition (PVD) process used for depositing materials onto a substrate, by ejecting atoms from such materials and condensing the ejected atoms onto a substrate in a high vacuum environment.

The basic process is as follows. A target, or source of the material desired to be deposited, is bombarded with energetic ions, typically inert gas ions such as Argon (Ar^+). The forceful collision of these ions onto the target ejects target atoms into the space. These ejected atoms then travel some distance until they reach the substrate and start to condense into a film. As more and more atoms coalesce on the substrate, they begin to bind to each other at the molecular level, forming a tightly bound atomic layer. One or more layers of such atoms can be created at will depending on the sputtering time, allowing for production of precise layered thin-film structures.

Though the basic idea of operation is seemingly simple, the actual mechanisms at play are quite complex. Electrically neutral Argon atoms are introduced into a vacuum chamber at a pressure of 1 to 10 m Torr. A DC voltage is placed between the target and substrate which ionizes Argon atoms and creates a plasma, hot gas-like phase consisting of ions and electrons, in the chamber. This plasma is also known as a glow discharge due to the light emitted. These Argon ions are now charged and are accelerated to the anode target. Their collision with the target ejects target atoms, which travel to the substrate and eventually settle. Electrons released during Argon ionization are accelerated to the anode substrate, subsequently colliding with additional Argon atoms, creating more ions and free electrons in the process, continuing the cycle.

6.1.2 Magnetron Sputtering Process

There are a number of ways to enhance this process. One common way to do this is to use what is known as a magnetron sputtering system. The main difference between this and a basic DC sputtering system, described above, is the addition of a strong magnetic field near the target area. This field causes traveling electrons to spiral along magnetic flux lines near the target instead of being attracted toward the substrate, Fig. 6.2. The advantage of this is that the plasma is confined to an area near the target, without causing damages to the thin film being formed. Also, electrons travel for a longer distance, increasing the probability of further ionizing argon atoms. This tends to generate stable plasma with high density of ions. More ions mean more ejected atoms from the target, therefore, increasing the efficiency of the sputtering process. The faster ejection rate, and hence deposition rate, minimizes impurities to form in the thin-film, and the increased distance between the plasma and substrate minimizes damage caused by stray electrons and argon ions.

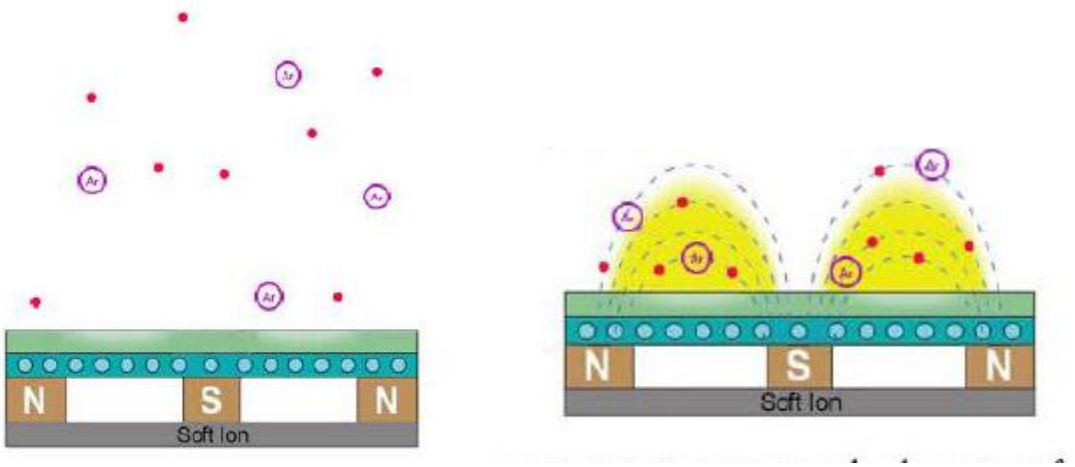

Figure 6.2.Comparison between a sputtering system and a magnetron sputtering system [1].

6.2 Experimental setup and testing procedure:

6.2.1 Pre-Sputtering procedure

Before fabricating the filter, pre-sputtering process was carried on. The glass was cleaned in an acetone, rinsed in de-ionized water several times and then inserted into the sputtering chamber. The substrate temperature and the chamber pressure were maintained at room temperature and 6.5×10^{-4} pa, respectively. The distance between the sputtering target and the substrate was about 5 cm.

The sputtering gas, which was used in the system, was argon (Ar). The sputtering chamber was heated to 350 $^{\circ}$C for 60 minutes before the sputtering process, to get rid of the water vapor at the walls and also to improve the film adhesion on the substrate. Table 6.1 shows the details of the pre-sputtering procedure before each run.

Table 6.1 Pre- sputtering procedure.

Flow Rate (SCCM)	Target	Base Pressure (pa)	Operating Pressure (pa)	Time (min)
30	ITO	6×10^{-4}	6.5×10^{-4}	60
30	SiO2	6×10^{-4}	6.5×10^{-4}	60
30	Si	6×10^{-4}	6.5×10^{-4}	60

6.2.2 Fabrication of the filter

Indium tin oxide (ITO), silicon (Si) and silicon dioxide (SiO_2) were used as sputtering targets. The glazing consists of ITO layer and four pairs of Si/ SiO_2 layers, deposited on top of a 1mm-glass sheet. The magnetron sputtering system was used to deposit a thin film from sputtering targets onto the substrate.

Figure 6.3 shows the sputtering targets after been deposited onto a substrate. The sputtering power was kept at 100W for both of the indium tin oxide and silicon, and 140W for silicon dioxide, to obtain a desired layer. The operation pressure was kept at 6×10^{-4}Pa.

Firstly, indium tin oxide was deposited on top of a 1mm-glass sheet substrates for 10 minutes and then alternating layers of Si/ SiO_2were deposited on top of the ITO. Si and SiO_2were deposited at different thicknesses, for comparison with the simulation. The amount of material sputtered from the target and deposited onto the substrate and the deposition time was recorded. The relationship between the thickness and the sputtering time are shown in Table 6.2, 6.3and Fig.6.4 (a), (b).

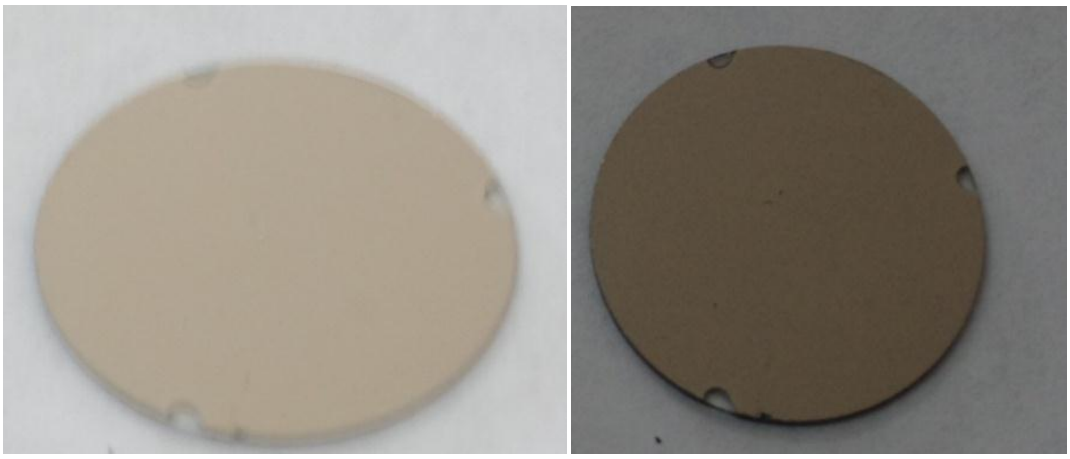

Fig.6.3: the deposited sputtering targets on a substrate which was used in the experiments: Si (left) and SiO_2 (right).

Table 6.2: Relation between thickness and sputtering time

Thickness (SiO_2) μm	0.1	0.15	0.2	0.22	0.3	0.32	0.35	0.39	0.4
Time(hour)	1	1.74	2.53	2.86	3.97	4.29	4.63	5.39	5.56

Table 6.3: Relation between thickness and sputtering time

Thickness (Si) μm	0.1	0.11	0.12	0.13	0.14	0.15	0.16	0.18	0.2
Time(hour)	0.26	0.50	0.75	0.96	1.12	1.36	1.61	1.99	2.47

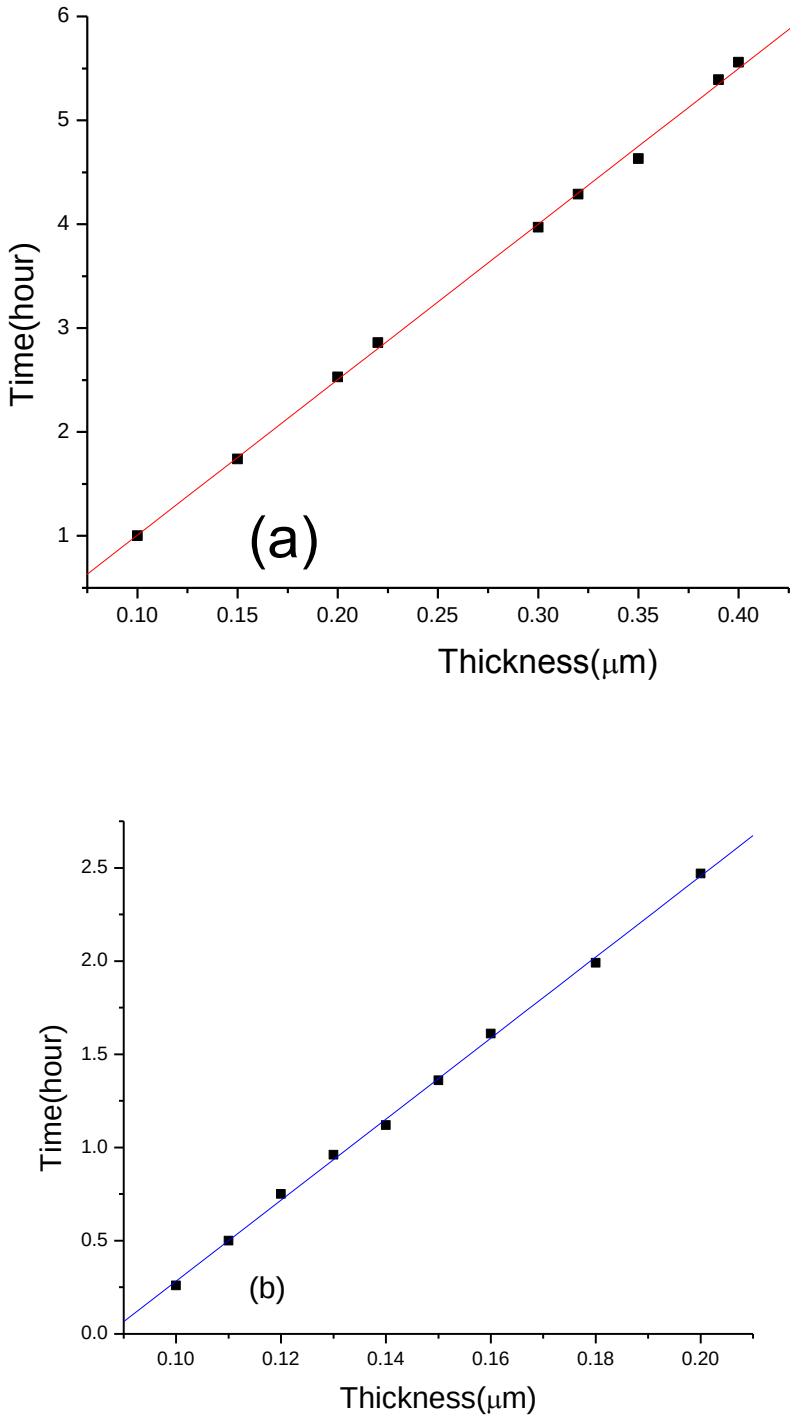

Figure6.4: Relation between thickness and time (a) SiO_2,(b)Si .

5.2.3 Measurement of the reflectance and transmittance:

The spectral transmittance and reflectance system consists of a powering system, light source, stepper motor, photo-detectors and analog to digital converter. The powering system consists of the power source (240 V a.c), 240V to 48 V step down transformer, full wave rectifier, two capacitors and two biasing resistors. It is shown in Figure. 6.6. The light source consists of a fluorescent lamp (250V, 25W) and a holographic grating (1200 lines/mm), which is placed in focus to the light. A concave mirror of focal length 5 cm mounted on a shaft of a gear system driven by a stepper motor of resolution 3.75°, focuses monochromatic beams vertically on the sample. The focusing concave mirror was mounted to a unipolar stepper motor, power rated (500mA, 24V), which was used to control small angle of rotations of the mirror. The first photo-detector receives the beam through computer controlled small angular rotations of the stepper motor. The reflected monochromatic beam from the probed thin film sample is directed to the second photo-detector and the intensities of both the incident and reflected beam are then converted to digital form by analog to digital converter, connected to enhanced parallel port used in computer interfacing. The spectral transmittance and reflectance instruments, used in this work at the Institute of Technology Laboratory, South Africa, are shown in Figure 6.7.

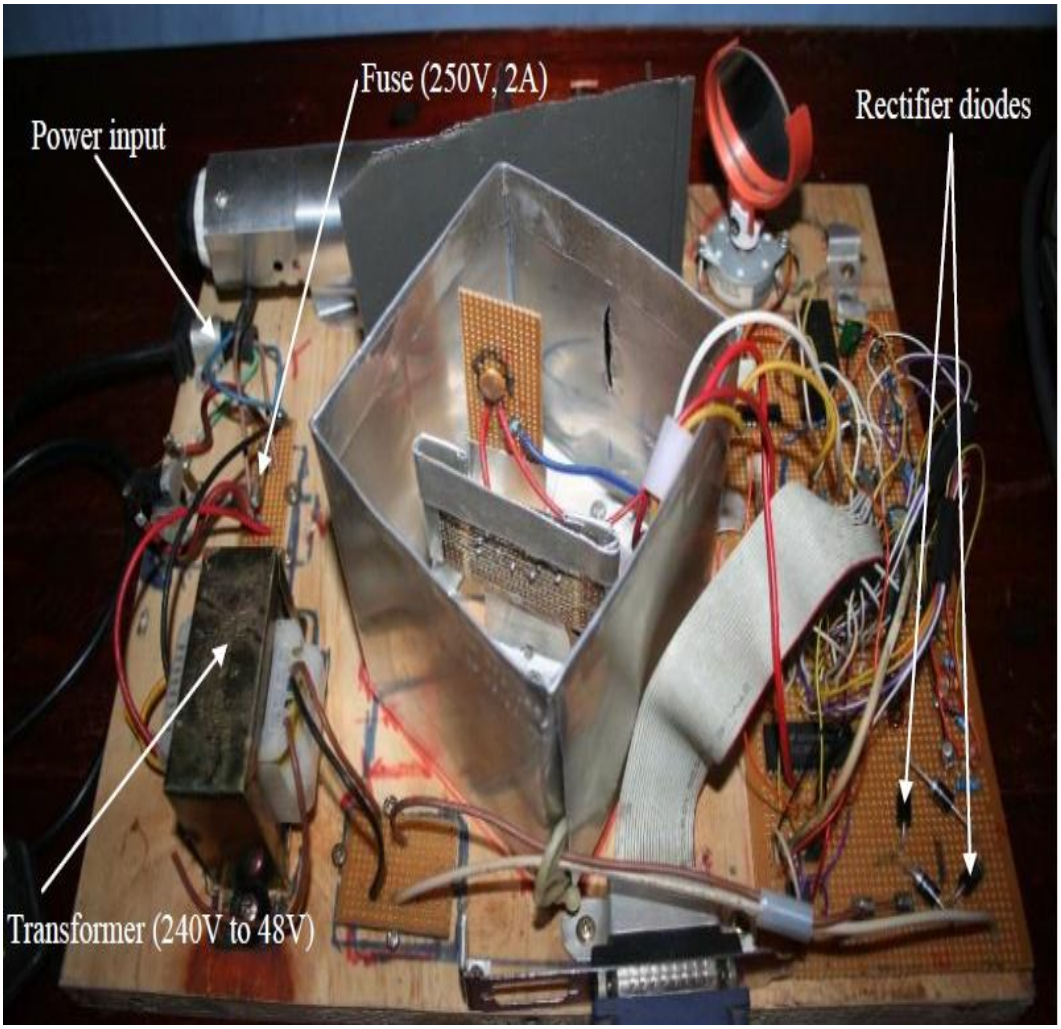

Figure 6.6: The powering system of the portable spectrometer.

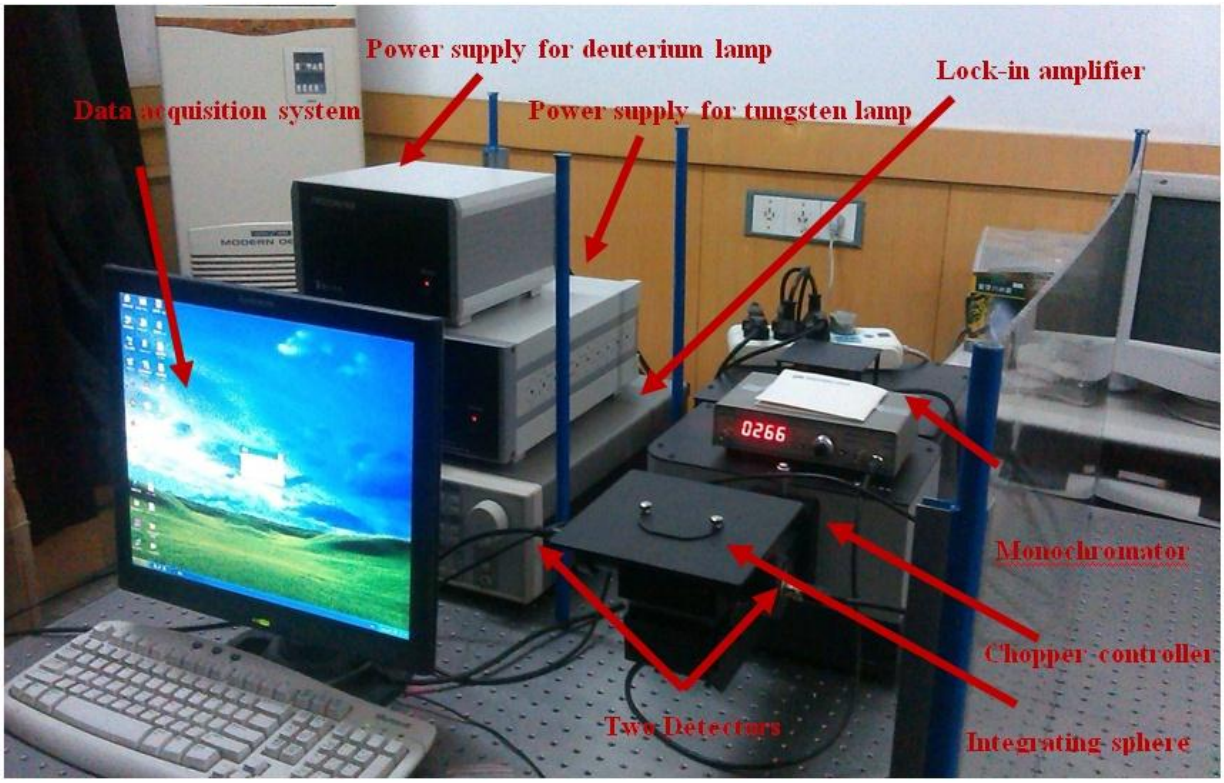

Figure. 5.7: Spectral transmittance and reflectance instrument located in the laboratory of the Institute of Technology, South Africa.

Chapter Seven

Result and Discussions

7.1 Introduction

The results of the simulation have shown that it is possible to design a filter which transmits most of the visible light and reflects the infrared radiation. In order to confirm that, the filter was fabricated at the University of Witwatersrand, South Africa. We discuss in this chapter the experimental results and compare it with the simulation results.

7.2Experimental Results

The filter has been fabricated by magnetron sputtering technique. The spectral transmittance and reflectance were measured by a system consisting of a powering system, light source, stepper motor, photo-detectors and analog to digital converter. The results of the measurement of the reflectance and transmittance are shown in Figure.7.1.The thickness of the Si, d, was taken to be 0.1, 0.15 and 0.4μm. The thickness of $SiO_2$was fixed at 0.4μm and that of ITO at 0.1μm.The results show that the optimum thickness for Si is 0.15μm. This agrees with the simulation results.

When using the optimum thickness of Si, the filter transmitted about 78% of the visible light and reflected nearly all the infrared radiation. The values are similar to that from the simulation results.

The experimental results confirmed that the filter can easily be fabricated and that it satisfies the thermal comfort of the occupants of the buildings. By transmitting most of the visible light and reflecting most of the heat, it reduces the electricity

consumption for lighting and cooling. During the night, in winter, it could act asan insulator to reflect the heat back inside the room. It satisfies the conditions for thermal comfort in both the hot days of summer and the cold nights of winter.

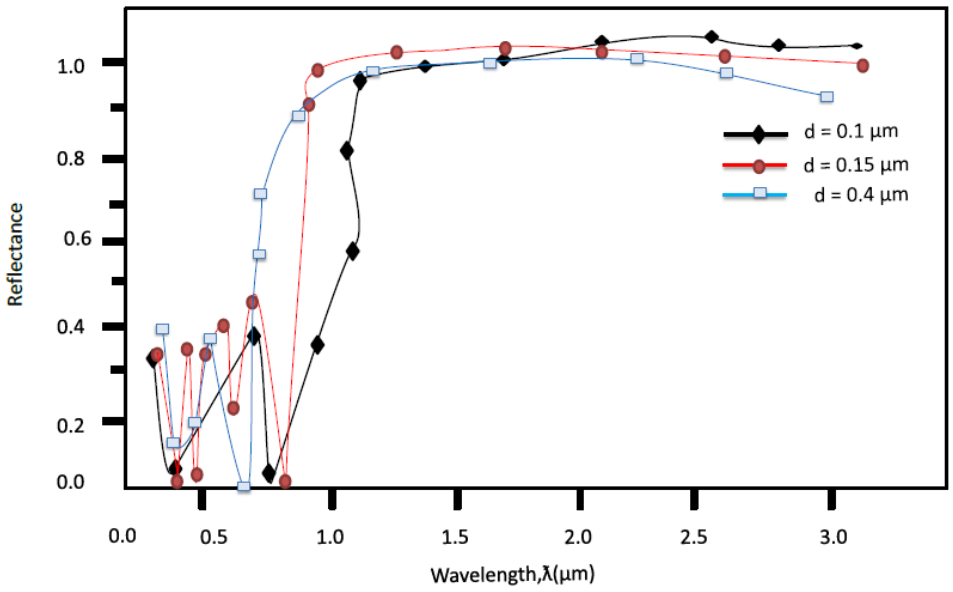

(a)

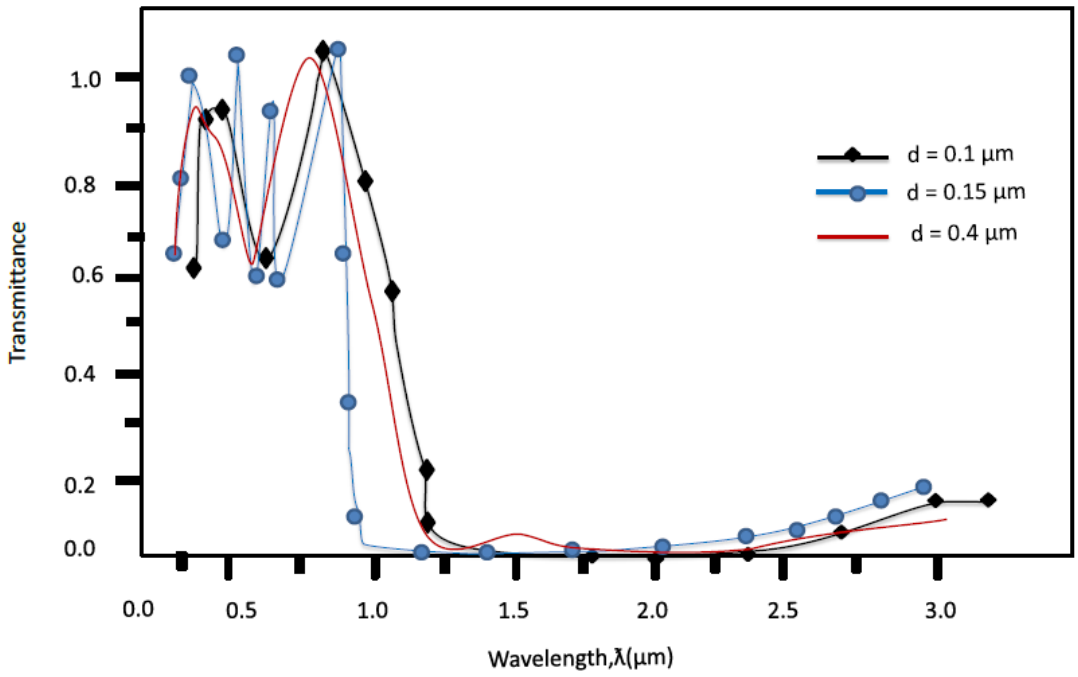

(b)

Figure.7.1: Reflectance and transmittance of the filter.

Chapter Eight

Conclusion and Recommendation

8.1 Conclusion

The thermal comfort temperature in Khartoum is between 31 and 27 ^{0}C. This could be achieved with minimum consumption of electricity. The windows represent the weakest point in the thermal performance of buildings. We have shown that it possible to control the optical performance of windows to transmit visible light and reflect the infrared. We have used Rigorous coupled-wave analysis (RCWA) to design a relatively simple and efficient glazing for hot climates. The glazing consisted of ITO and four periodic pairs of Si/SiO_2, deposited on a glass sheet.

RCWA was used to calculate the reflectance and transmittance of the different thicknesses of the layers. The optimum thicknesses of ITO, Si and SiO_2 were found to be (in both simulation and experimental work) 0.1 μm , 0.15 and o.4μm, respectively. The glazing transmitted 78% of the visible light and reflected almost all the infrared radiation from the sun. The optical properties of the glazing hardly depended on the angle of incidence of solar radiation. This makes it ideal for all hours of the day. During the night, in winter, it could act as an insulator to reflect the heat back inside the room. It satisfies the conditions for comfort in both the hot days of summer and the cold nights of winter.

The preparation of the filter and the testing were performed at the laboratories of the Faculty of Science, University of Witwatersrand, South Africa. Indium tin oxide (ITO), silicon (Si) and silicon dioxide (SiO_2) were used as sputtering targets.

The magnetron sputtering system was used to deposit a thin film from sputtering targets onto the substrate.

The transmittance and reflectance of the filter were measured by a system consisting of a powering system, light source, stepper motor, photo-detectors and analog to digital converter.

The experimental results were found to be in good agreement with the simulation results. The results make the filter attractive for future commercialization.

It can be concluded that the proposed filter has the advantage that it is relatively simple, efficient, and compared with commercial smart windows, it does not need any external source of energy to control its optical properties. It can be used in hot climates in buildings and vehicles.

8.2 Recommendations for Future Work

The proposed selective filter needs to be tested in real conditions. The electricity consumption for cooling and lighting is to be measured in two typical rooms, one with ordinary windows and the other with the selective filter. The economics of the energy saving and the payback period can then be determined.

References:

1. J.A. Duffie and W.A. Beckman, Solar Engineering of Thermal process, John Wile and sons Inc, USA, 1991.

2. R. A. Messenger and J.Ventre, Photovoltaic systems engineering, C R C Press, New York , 2004 .

3. Ministry of Water Resources, Irrigation and Electricity, Khartoum, Sudan, 2015.

4. Info@climatestotravel.com.

5. American Society of Heating, Refrigerating and Air-Conditioning Engineers (ANSI/ASHRAE), Inc., Thermal Environmental Conditions for Human Occupancy (2010).

6. Ricardo Forgiarini Rupp, Natalia GiraldoVásquez and Roberto Lamberts, Energy and Buildings 105(2015) 178–205.

7. Mohammad Taleghani, MartinTenpierik, StanleyKurvers and Andy van den Dobbelsteen, Renewable and Sustainable Energy Reviews 26(2013)201–215.

8. Aihua Mao, JieLuo and Yi Li, Applied Thermal Engineering 117 (2017) 629–643.

9. Letizia Martinelli, Tzu-Ping Lin and Andreas Matzarakis, Building and Environment 92 (2015) 30e38.

10. FerdinandoSalata, IacopoGolasi, DavidePetitti, Emanuele de LietoVollaro, Massimo Coppi and Andrea de Lieto Vollaro, Sustainable Cities and Society 30 (2017) 79–96.

11. Andrew M. Coutts & Emma C. White & Nigel J. Tapper & Jason Beringer & Stephen J. Livesley, Theor Appl Climatol (2016) 124:55–68.

12. S. Rudolph et al. / Ashrae Journal, July (2009) 104-107.

13. S. Hong and L. Chen, Solar Energy Materials & Solar Cells 104 (2012) 64-74.

14. S. Kim and M. Taya, Solar Energy Materials & Solar Cells 107 (2012) 225-229.

15. S. Kim, X. Kong and M. Taya, Solar Energy Materials & Solar Cells 117 (2013) 183-188.

16. M. Fernandes, V. T. Freitas, S. Pereira, E. Fortunato, R.A.S. Ferreira, L.D. Carlos, R. Rego, V. Bermudez, Solar Energy Materials & Solar Cells 123 (2014) 203-210.

17. W. J.Hee, M.A. Alghoul, B. Bakhtyar, E. OmKalthum, M. A. Shameri, M. S. Alrubaih, K. Sopian,Renewable and Sustainable Energy Reviews 42 (2015) 323-343.

18. R. Brooke, M. Fabretto, N. Vucaj, K. Zuber, E. Switalsaka, L. Reeks, P. Murfy and D. Evans, Smart Mater. Struct. 24 (2015) 035016.

19. E. Kim, I. Choi, J. Oh, Y. Kim, J. Lee, Y. Choi, J. Cho, Y. Kim and G. HEO, Japanese Journal of Applied Physics 53 (2014) 095505.

20. H. Khandelwal, R. Loonen, J. Hensen, M. Debije and A. Schenning, Scientific Reports 5 (2015) 11773.

21. J. Wang, L. Zhang, L. Yu, Z. Jiao, H. Xie, X. W. Lou, X. W. Sun, Nature Communications 5921 (2014).

22. S. H. N. Lim, J. Isidorsson, L. Sun, B. L. Kwak and A. Anders,Solar Energy Materials & Solar Cells 108 (2013) 129-135.

23. RanjitA.Patil, RupeshS.Devan, YungLiou and Yuan-RonMa, Solar Energy Materials & Solar Cells 147 (2016) 240-245.

24. L. Long, H. Ye, H. Zhang and Y. Gao, Solar Energy 120 (2015) 55-64.

25. Linshuang Long, Hong Ye, Haitao Zhang and YanfengGao, Solar Energy Materials & Solar Cells 120 (2015) 55–64.

26. JianyunZheng, ShanhuBao and Ping Jin, Nano Energy 11 January 2015.

27. H. Koo, D. Shen, S. Bae, K. Ko, S. Chang and C. Park, Journal of Material Engineering and Performance 23 (2014) 402-407.

28. M. Kamalisarvestani, R. Saidur, S. Mekhilef, F.S. Javadi, Renewable and Sustainable Energy Reviews 26 (2013) 353–364.

29. Y. Mouedden et al. Proceeding of 9th International Conference (HONET) (2012) 83-86 Istanbul, Turkey.

30. S. G. Babiker et al/ WSEAS Transactions on Applied and Theoretical Mechanics 9 (2014)97-103.

31. C. Batista, R. Ribero and V. Teixeira, Nanoscale Research Letters (2011) 6:301.

32. Linshuang Long and Hong Ye, Solar Energy Materials & Solar Cells 107 (2014) 236–244.

33. J.Zhou, Y. Gao, Z. Zhang, H. Luo, C. Cao, Z. Chen, L. Dai and X. Liu, www.nature.com/scietificreports 3:3029 (2013).

34. WeiFeng, LipingZou, GuohuaGao, GuangmingWu, JunShen and WenLi,Solar Energy Materials & Solar Cells 144 (2016) 316-323.

35**.** S. G. Babiker, Y. Shunai, M. O. Sid-Ahmed, M. Xie, WSEAS Transactions on Applied and Theoretical Mechanics 9 (2014) 97-103.

36. M.G. Moharam, and K.T. Gaylord, "Rigrous coupled-wave analysis of planar-grating diffraction," Opt. Express, 71 (1981)811-818.

37. S. Peng and M.G. Morris, "Efficient implementation of rigorous coupled-wave analysis for surface-relief gratings," Opt. Express, 12 (1995)1087-1096.

38. D.E. Palik, "Handbook of Optical Constants of Solids," Academic Press, San Diego, CA, 1985.

39. Mattox, Handbook of Physical Vapor Deposition (PVD) Processing: Film Formation, Adhesion, Surface Preparation and Contamination Control. Park Ridge, New Jersey: Noyes Publications, (1998).
40. https://infogalactic.com/info/Scanning_electron_microscope
41.http://www2.chemistry.msu.edu/faculty/reusch/VirtTxtJml/Spectrpy/UVVis/spectrum.htm
42. Skoog, et al. Principles of Instrumental Analysis. 6th ed. Thomson Brooks/Cole. 2007, 349-351.
43. Horie, M.; Fujiwara, N.; Kokubo, M.; Kondo, N.Spectroscopic thin film thickness measurement system for semiconductor industries,Proceedings of Instrumentation and Measurement Technology Conference, Hamamatsu, Japan, 1994,(ISBN 0-7803-1880-3).
44. Sadtler, Handbook of UV spectra, Heyden, London, 1979
45. Chang, Raymond. Physical Chemistry for the Biosciences. USA: University Science Books, 2005.
46. Gore, Michael. Spectrophotometry & Spectrofluorimetry. New York: Oxford University Press, 2000.
47. Price, Nicholas and Dwek, Raymond and Wormald, Mark. Principles and Problems in Physical Chemistry for Biochemists. R. G. Ratcliffe. New York: Oxford University Press, 1997.